

ENGINEERING RESEARCH INSTITUTE
UNIVERSITY OF MICHIGAN
ANN ARBOR

SPACE-CHARGE EFFECTS AND FREQUENCY CHARACTERISTICS
OF C-W MAGNETRONS RELATIVE TO THE PROBLEM OF FREQUENCY MODULATION

Technical Report No. 1
Electron Tube Laboratory
Department of Electrical Engineering

BY

H. W. WELCH, JR.

Approved By:



Gunnar Hok



W. G. Dow

Project M694

For

CONTRACT NO. W-36-039 sc-32245
SIGNAL CORPS, DEPARTMENT OF THE ARMY
DEPARTMENT OF ARMY PROJECT NO. 399-13-022
SIGNAL CORPS PROJECT NO. 112B-0

November 15, 1948

Einige

UMKÖSIZ

ENGIN.
9.84
9-13-55

i

TABLE OF CONTENTS

	<u>Page</u>
PERSONNEL OF UNIVERSITY OF MICHIGAN ELECTRON TUBE LABORATORY	ii
ABSTRACT	iii
ACKNOWLEDGMENTS	iv
1. INTRODUCTION	1
2. EQUIVALENT CIRCUIT	3
3. EXPERIMENTAL EVIDENCE OF SPACE-CHARGE EFFECTS ON FREQUENCY CHARACTERISTICS	7
4. SPACE CHARGE AND THE EQUIVALENT CIRCUIT	24
5. ANALYSIS OF SPACE-CHARGE BEHAVIOR	26
Case I - The Non-Oscillating Magnetron, No R-F Voltage Present	28
Case II - Non-Oscillating Magnetron with R-F Voltage Applied From External Source	34
6. PROPAGATION OF THE ELECTROMAGNETIC WAVE IN THE MAGNETRON SPACE CHARGE	42
7. DISCUSSION OF SPACE-CHARGE BEHAVIOR AND INTERPRETATION OF EXPERIMENTAL EVIDENCE	57
a. Hull Voltage: Noise in Magnetrons	59
b. Hartree Voltage: Oscillation	60
c. Frequency Pushing	62
d. Space-Charge Effects on Rieke Diagram	63
e. Hot Impedance Measurements	64
8. GENERAL DISCUSSION OF FREQUENCY MODULATION METHODS: DESIGN CRITERIA FOR MULTIANODE STRUCTURES	72
9. SUGGESTED GEOMETRIES FOR F-M MAGNETRONS	77
10. CONCLUSIONS	87
BIBLIOGRAPHY	91
DEFINITIONS OF SYMBOLS	96

PERSONNEL OF UNIVERSITY OF MICHIGAN
ELECTRON TUBE LABORATORY

Scientific and Engineering Personnel

W. G. Dow	Professor of Electrical Engineering	Supervisor
H. W. Welch	Research Physicist	Full time
J. R. Black	Research Engineer	Full time
G. Hok	Research Engineer	1/4 time
R. K. Brown*	Research Engineer	1/2 time
R. Callahan*	Research Associate, Student	1/2 time
G. R. Brewer	Research Assistant, Student	1/3 time
C. K. Birdsall*	Research Assistant, Student	1/3 time

Service Personnel

V. R. Burris	Machine Shop Foreman	Full time
R. F. Steiner	Assembly Technician	Full time
Mrs. G. R. Merithew	Draftsman and Illustrator	3/4 time
G. Sabedash	Machinist	1/4 time

* These personnel were involved in compilation of material included in this report, but are no longer with the project.

ABSTRACT

The major purpose of this report is to integrate and supplement the knowledge of space-charge effects and frequency characteristics of c-w magnetrons into a more useful tool for attacking the problem of analysis and control of these properties.

The methods of analysis and the experimental data which have bearing on the problem of c-w magnetrons are discussed in their relation to each other and in their relation to the problem of frequency modulation. Major emphasis is on the quantitative interpretation of "hot impedance" measurements made on the pre-oscillating magnetron. The results of the analysis of these measurements, which give an improved understanding of space-charge behavior, are related to the Hull and Hartree voltage boundaries and, qualitatively, to the phenomena of frequency pushing and frequency pulling.

Various methods of frequency modulation are discussed and specific methods proposed.

Several curves, relating dimensionless variables which are useful in calculations involving the magnetron space charge are presented.

ACKNOWLEDGMENTS

Every member of the staff of the University of Michigan Tube Laboratory was involved in the preparation of the material used in this report. Mr. Gunnar Hok was especially helpful in his careful criticism of the analysis and presentation. The work was supervised by Professor W. G. Dow who was originally responsible for the emphasis in this laboratory on the method of hot impedance testing used in experimental analysis of the magnetron space charge. The method used in calculation of the Hartree voltage was suggested by Professor Dow in regular lectures of a course on microwave electron tubes.

SPACE-CHARGE EFFECTS AND FREQUENCY CHARACTERISTICS
OF C-W MAGNETRONS RELATIVE TO THE PROBLEM OF FREQUENCY MODULATION

1. INTRODUCTION

The purpose of this report is threefold: to summarize in one place the available knowledge of frequency characteristics of c-w magnetrons with particular reference to space-charge effects; to present analysis and experimental data which give insight into the problem of frequency modulation of c-w magnetrons; and to suggest methods of application of these ideas, some of which will be attempted in the University of Michigan Laboratory in the near future.

The complete discussion of frequency characteristics of c-w magnetrons requires attention to a varied subject matter. Much of this subject matter has been treated in reports of government agencies and in the journals and is generally understood. There are, however, several points at which present knowledge becomes inadequate background for an understanding of the mechanism of magnetron operation. This is particularly the case when one is to predict quantitatively the behavior of magnetron space-charge clouds under the influence of strong r-f fields.

The circuital aspects of magnetron frequency characteristics are generally treated by establishment of an equivalent circuit and interpretation of that equivalent circuit in terms of experimentally measurable quantities. The most conveniently measurable quantities are resonance wavelength, loaded Q and minimum standing-wave ratio. The

relationships between these quantities and other, unmeasurable quantities in the equivalent circuit are fairly well defined and understood. This theory can be extended to explain semi-quantitatively effects of the output circuit and load on magnetron frequency characteristics such as frequency pulling and long-line effect.

Frequency characteristics of an operating magnetron must be obtained from the following types of experimentally obtained information: Rieke diagrams, relating frequency of oscillation and power output to load characteristics; frequency pushing measurements, relating frequency and plate current for constant loading; and modulation characteristics determined by spectral measurements of various types. Interpretation of these types of data depends on knowledge of the physics of space-charge effects in the oscillating magnetron and, at this point, is almost entirely qualitative.

The means of frequency modulation of a magnetron electronically may be divided into four categories. One, the modulation is obtained through effects due to the same electrons that are the source of oscillation. Two, reactive effect due to electrons in a structure external to the magnetron resonant circuit and separate from the load is coupled into the circuit. Three, frequency pulling is utilized by electronic variation of the load impedance. Four, a second source of electrons is introduced into the resonant circuit in such a way as to produce a controllable reactive effect. In any of the last three of these methods a physical means for effectively introducing and controlling the electron beams or clouds must be devised. The theory of the behavior of beams has been worked out with satisfactory results. The behavior of electron clouds has been studied in some detail in connection with the theory of

magnetron operation, but quantitative methods of predicting effects on frequency under the conditions of high r-f field are still not available.

One approach to the f-m problem on first inspection seems to have greater possibilities than the others for giving large frequency shifts resulting from electronically introduced reactance. This is to utilize the relatively high space-charge density of the magnetron-type rotating cloud in devices of the fourth category mentioned above. That is, the electronic reactance is incorporated within the resonant circuit of the magnetron. A program of experimentation intended to supplement efforts of theoretical nature toward a better understanding of magnetron space-charge reactance has been started. Impedance measurements are made on hot magnetrons at plate voltages below that required to initiate oscillation. Structures suitable for introducing reactive effects of rotating space-charge clouds into a magnetron resonant circuit are devised. Operating behavior of these devices will furnish further information.

Two problems intimately associated with the practical use of frequency-modulated magnetrons are frequency stabilization and reduction of noise level. The former is primarily a problem of engineering while the latter is a problem which will require better understanding of the basic physics in a magnetron before positive steps can be taken. The group at the University of Michigan is not at present actively concerned with work of this nature, but it is necessary to keep in mind the limitations which may be imposed.

2. EQUIVALENT CIRCUIT

The details of an equivalent circuit for a microwave device such as a magnetron naturally change with the structure of the magnetron.

Effects of end hats, straps, cathode-supporting structures, etc., may or may not be important enough to be included in the circuit. The equivalent circuit is usually based on the assumption that the various possible modes of oscillation are sufficiently separated in frequency to be considered individually. This permits the representation of the resonant circuit of the magnetron as a simple parallel resonant circuit. When this assumption is not valid, the resonance is made complex and, in general, must be treated as a special case. However, if the assumption is not justified, some sort of device is usually necessary to induce mode separation before the magnetron is practically usable. Thus, in most practical cases, the simplified approach is adequate.

The most important concept in connection with equivalent circuits of magnetrons relative to the present problem is the concept of electron-transit admittance. It is the susceptive portion of this admittance which is usable as a frequency modulation device. If an equivalent circuit may be established in which the function of the electron-transit susceptance is properly understood, the picture is greatly simplified. This has been done satisfactorily for triodes, tetrodes and klystrons, but the picture in the case of magnetrons is still obscure. The circuit in Figure 1a is suggested as equivalent in the case of a non-oscillating magnetron. In this circuit, the electron-transit susceptance is represented by y_e which may be defined as the susceptance of the electrons as seen from terminals representing the two sets of anodes. The nature of this susceptance changes for various conditions of anode voltage, magnetic field and r-f voltage between anode segments. The primary purpose of this report is to present the overall picture of these changes. The picture for an oscillating magnetron is more complex. However, a convenient

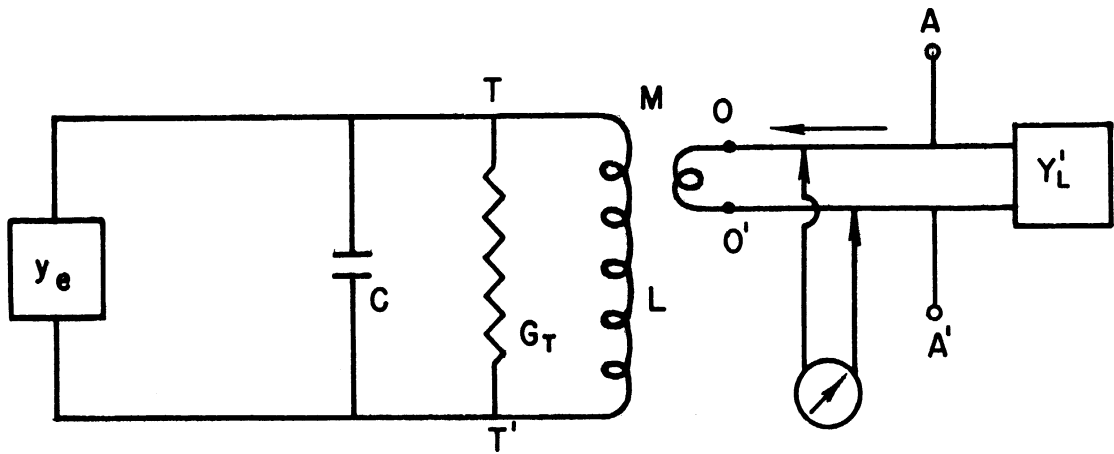


FIG Ia EQUIVALENT CIRCUIT FOR NON-OSCILLATING MAGNETRON

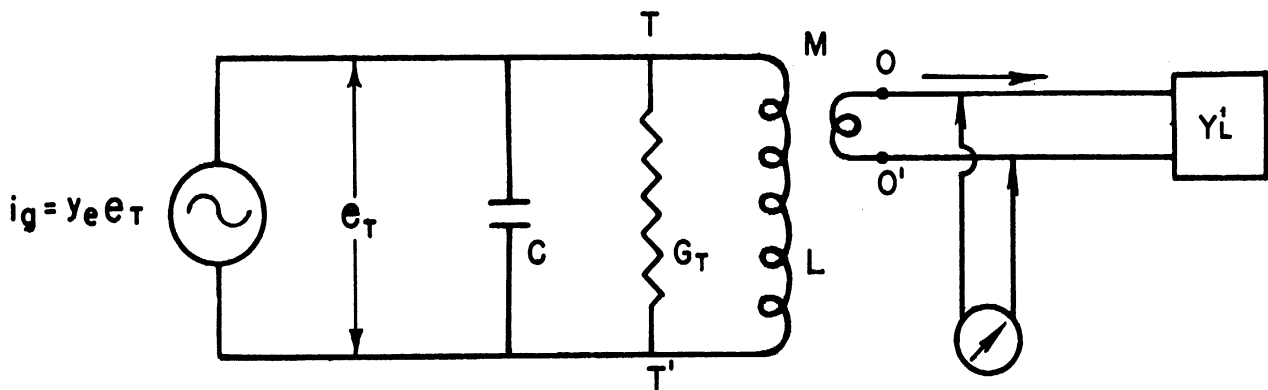


FIG Ib EQUIVALENT CIRCUIT FOR OSCILLATING MAGNETRON

FIG I EQUIVALENT CIRCUITS

ARROW INDICATES DIRECTION OF POWER FLOW

picture is obtained by replacing the admittance y_e by a current generator $i_g = y_e e_T$. The admittance y_e may now be thought of as the equivalent admittance of a current generator. The value of this admittance is a function of plate current and loading. We will show later that variation in this admittance with current is the cause of frequency pushing.

Experimental investigation of the nature of the quantity y_e must be made by a meter located in the line between the output terminals O, O' and the load Y_L . In the case of the non-oscillating magnetron (Figure 1a) an external signal must be fed into the circuit at the points A, A' . Measurements of standing-wave ratio and position of minimum coupled with a knowledge of properties of the circuit and the controllable parameters in the circuit yield an experimental result for y_e as a function of the variable parameters. This type of measurement we call a hot impedance test, in analogy with the established term, cold impedance test. When anode voltage is increased to the point of supporting oscillation, these measurements can no longer be made and the circuit in Figure 1b applies. Standing-wave ratio and position of the minimum measurements now apply to the load. No external source is present. The load is therefore used as a variable and the effect on resonance wavelength, power output, etc., is recorded in the Rieke diagram. Variation of frequency with plate current (frequency pushing) can be measured quite simply in connection with overall performance data taken for constant loading.

Discussion of established concepts having to do with the mechanics of equivalent circuits of this type will be found in the references⁽¹⁾. We will try in the following pages to give some clarification

(1) II-1; I-4; I-5, sec. 9; I-6, ch. 7; I-7, ch. 20.

to the meaning of the quantity y_e and its relation to methods of frequency modulation.

3. EXPERIMENTAL EVIDENCE OF SPACE-CHARGE EFFECTS ON FREQUENCY CHARACTERISTICS

The measurable frequency characteristics of magnetrons may be interpreted in terms of the equivalent circuit discussed in the last section. The various experimental data available are presented first without much analytical discussion for the purpose of summarizing the evidence of space-charge effects on frequency behavior. The effects which are observed may be used or avoided in methods of frequency modulation. In order to simplify the discussion, the circuits of Figure 2 will be used, in which the load is transformed to the terminals of the tank circuit, T, T'. This can be done if the mutual inductance M is known.

A typical Rieke diagram, showing the effect of the load impedance on magnetron operation is shown in Figure 3a. The experimental method used in obtaining this sort of data is well known and described in references provided for this section⁽¹⁾. This diagram is replotted in rectangular coordinates in Figure 3b. It will be noted that the power contours are approximately parallel to lines of constant load conductance while the frequency contours diverge from lines of constant load susceptance. The conditions for oscillation in terms of Figure 2b are the following:

$$\begin{aligned} \text{(a)} \quad g_e + G_T + G_L &= 0 \\ \text{(b)} \quad b_e + B_T + B_L &= 0 \end{aligned} \tag{3.1}$$

Here

$$g_e + jb_e = y_e \quad \text{the admittance of the space charge}$$

(1) III-1, p. 30; III-2; I-5, sec. 10.9; I-6, pp. 733-734.

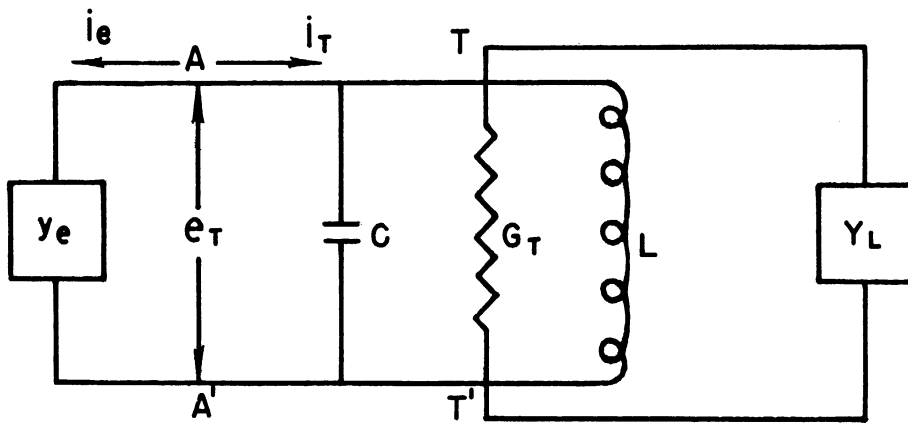


FIG. 2a SIMPLIFIED EQUIVALENT CIRCUIT
FOR NON-OSCILLATING MAGNETRON

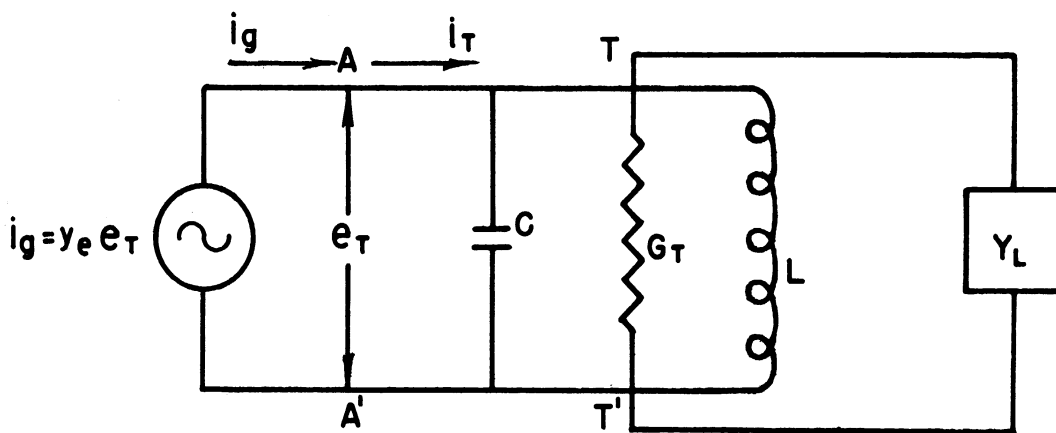


FIG 2b SIMPLIFIED EQUIVALENT CIRCUIT
FOR OSCILLATING MAGNETRON

FIG 2 SIMPLIFIED EQUIVALENT CIRCUITS

$G_T + jB_T = Y_T$ the admittance of the tank circuit

$G_L + jB_L = Y_L$ the admittance of the load transformed to the terminal T-T'

Assuming that b_e and B_L are small compared to the total tank-circuit susceptance (as is generally the case), the frequency of oscillation will be nearly equal to the cold resonant frequency of the circuit. In this case

$$B_T \cong 2Y_{oc} \frac{\omega_f - \omega_o}{\omega_o} \quad (3.2)$$

where

$$Y_{oc} = \sqrt{\frac{C}{L}}$$

ω_f = oscillatory frequency

ω_o = cold resonant frequency

From Equations 3.2 and 3.1

$$\frac{\omega_f - \omega_o}{\omega_o} = - \frac{1}{2} \frac{b_e + B_L}{Y_{oc}} \quad (3.3)$$

Thus, based on this simplified approach, ω_f is directly proportional to B_L . If ω_f were independent of G_L , as Equation 3.3 outwardly indicates, lines of constant frequency would coincide with lines of constant susceptance in the presentation of experimental data of Figure 3. The experimental results definitely indicate that there is a dependence of ω_f on G_L and consequently, from Equation 3.3, b_e must depend upon G_L . This is not at all surprising upon consideration of Equation 3.1. In order to maintain balance in Equation 3.1a as G_L is changed, g_e must change. G_T is relatively constant. It is almost inconceivable that negative conductance of the rotating space charge could change without a coincident change in susceptance. This change, when applied to Equation 3.1b, requires a shift in B_L to maintain constant frequency. Thus, the constant frequency contours in Figure 3 do not coincide with constant B_L contours.

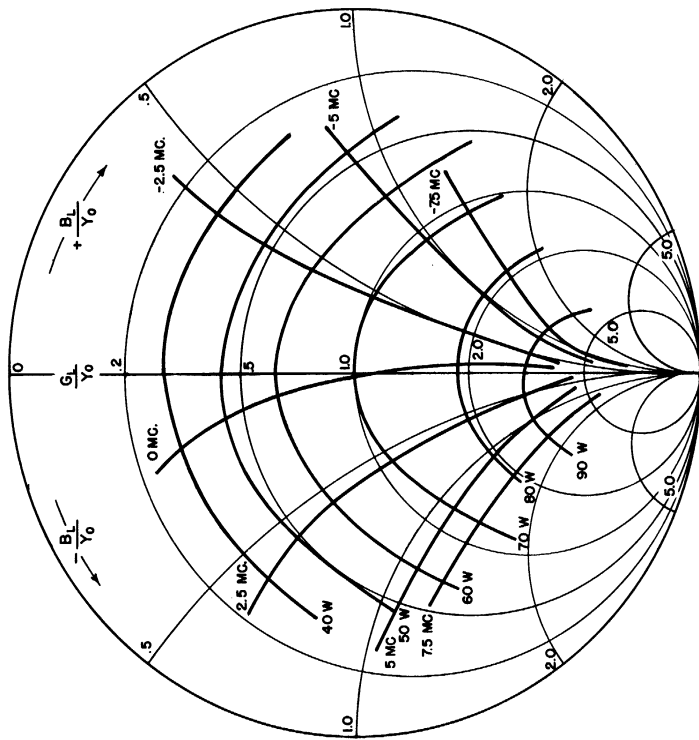


FIG 3a RIEKE DIAGRAM, SMITH CHART

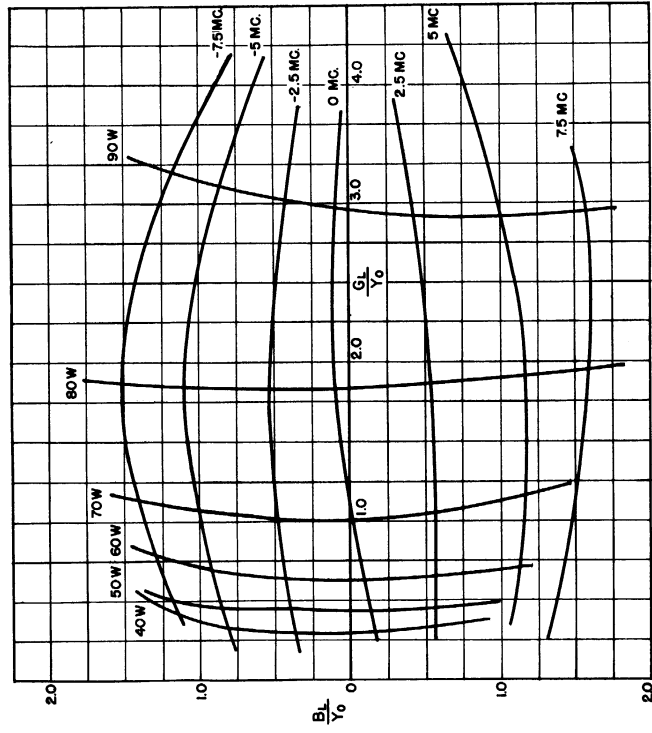


FIG 3b RIEKE DIAGRAM, CARTESIAN COORDINATES

FIG. 3 TYPICAL RIEKE DIAGRAM SHOWING DISTORTION OF FREQUENCY CONTOURS

In the case of klystrons the frequency contours are straight lines inclined at an angle to the lines $B_L = \text{constant}$. This would indicate that b_e is a linear function of g_e . However, the evidence in the case of magnetrons is not so conclusive.

The experimental fact important to the present discussion is that susceptance and conductance of the rotating space-charge cloud as seen from the anodes of a magnetron are interdependent. Frequency pulling, as usually defined⁽¹⁾, is also dependent upon this effect, but may be associated primarily with frequency variation due to changes in the susceptible portion of the load.

A second experimentally observed effect on frequency is the phenomenon of frequency pushing. Frequency pushing is defined as the variation in oscillator frequency as a function of plate current for constant loading and constant magnetic field⁽²⁾. Data are quite easily obtained simply by observing, with the aid of a spectrum analyzer or wave meter, frequency change as plate current is varied. A dynamic method in which plate current and wave meter pips are presented oscilloscopically is preferred. Shifts in frequency due to temperature effects are likely to invalidate measurements made statically. Typical frequency-pushing data are given in Figure 4. Resonant wavelength, frequency shift and plate current are plotted against plate voltage. Plate voltage is found to be a more useful parameter than plate current in the discussion of such data. The largest frequency change usually occurs for relatively low currents. Thus, if amplitude modulation without frequency modulation

(1) I-5, sec. 9.4.

(2) III-3; I-7, p. 506.

is desired, it is necessary to restrict the modulation to the order of 50 per cent. The expected frequency variation accompanying an amplitude modulation greater than 90 per cent is from .1 per cent to .2 per cent for a c-w magnetron, depending on the structure. Experimental evidence indicates that large frequency pushing may be associated with low Q or large pulling figure. However, because Q cannot be changed without affecting shunt impedance and field distribution, the correlation is not direct and cannot be used for quantitative predictions. Frequency behavior at very low currents does not tie in with even the simple qualitative theory because of the presence of other modes than the fundamental.

Modulation produced by the magnetic field variation due to alternating currents in the heater is a common source of trouble in c-w magnetrons. This effect is a form of frequency pushing. It is not particularly usable for modulation purposes. Where frequency stability is required, it must be eliminated by proper design of the heater structure or use of direct current in the heater.

There is a third type of data which appears on first examination to be most useful as an aid to the understanding of space-charge behavior and to the development of frequency-modulation devices. These are the data resulting from measurements made on magnetrons in which electrons are circulating but not reaching the anode. The method of measurement is the same as that used for cold impedance tests on microwave tubes and resonant cavities. In order to differentiate the term "hot impedance test" is used, implying that the magnetron is "hot" and capable of drawing plate current if the conditions of anode voltage and magnetic field are properly adjusted. The various conditions under which data may be taken give a wide range of possibilities for interpretation. Variations of Q_0 ,

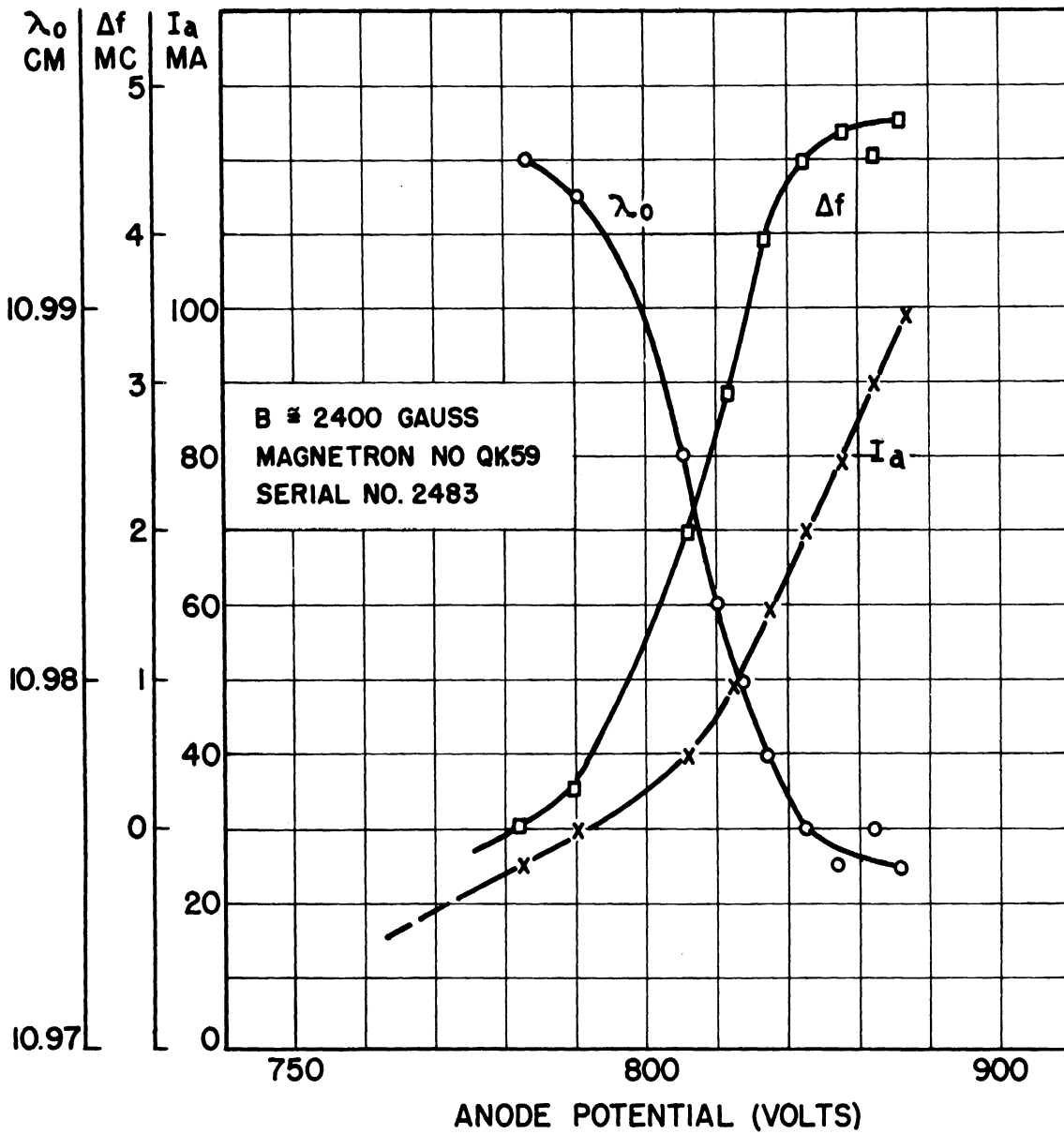


FIG. 4 TYPICAL FREQUENCY PUSHING CURVE

λ_0 and G_0 with plate voltage have been investigated at several values of input r-f voltage. Q_0 is the unloaded Q of the magnetron, λ_0 is the resonant wavelength and G_0 is the input conductance at resonance. $G_0 = Y_0/\sigma_0$ where σ_0 is the minimum standing-wave ratio and Y_0 is the characteristic admittance of the line. In order to approximate conditions achieved in a frequency modulation device, measurements at high r-f voltages are desirable. To accomplish this, one magnetron may be used to drive another. A schematic drawing of such an experimental setup is shown in Figure 5. R-f voltage is varied by means of attenuating reflectors placed in a slotted section between the impedance matching load and the magnetron under investigation. R-f voltage is measured by a probe placed at a voltage minimum (at cold resonance) approximately 3 wavelengths from the magnetron coupling loop (L_M in the diagram). This probe leads to a crystal detector and micro-ammeter. The probe is calibrated against power measurements into a matched load and r-f voltage calculated from the known line impedance of 52 ohms. The impedance-matching load is quite useful for measurements of this type or in any application where a high-Q circuit is to be driven by a magnetron. It consists of two loads separated by $\lambda/4$. The driving magnetron is thus under no circumstances subjected to standing-wave ratios greater than 3 to 1.

The results of hot impedance measurements made under various conditions are shown in Figures 6, 7, 8, 9 and 10. Figure 6 compares hot impedance results in the pre-oscillation region with the frequency pushing data of Figure 4. The two sets of data were taken under the same conditions on the same magnetron. The magnetic field is such that oscillation begins about 750 volts. Note that the wavelength becomes greater until oscillation starts. At this point the direction of the shift

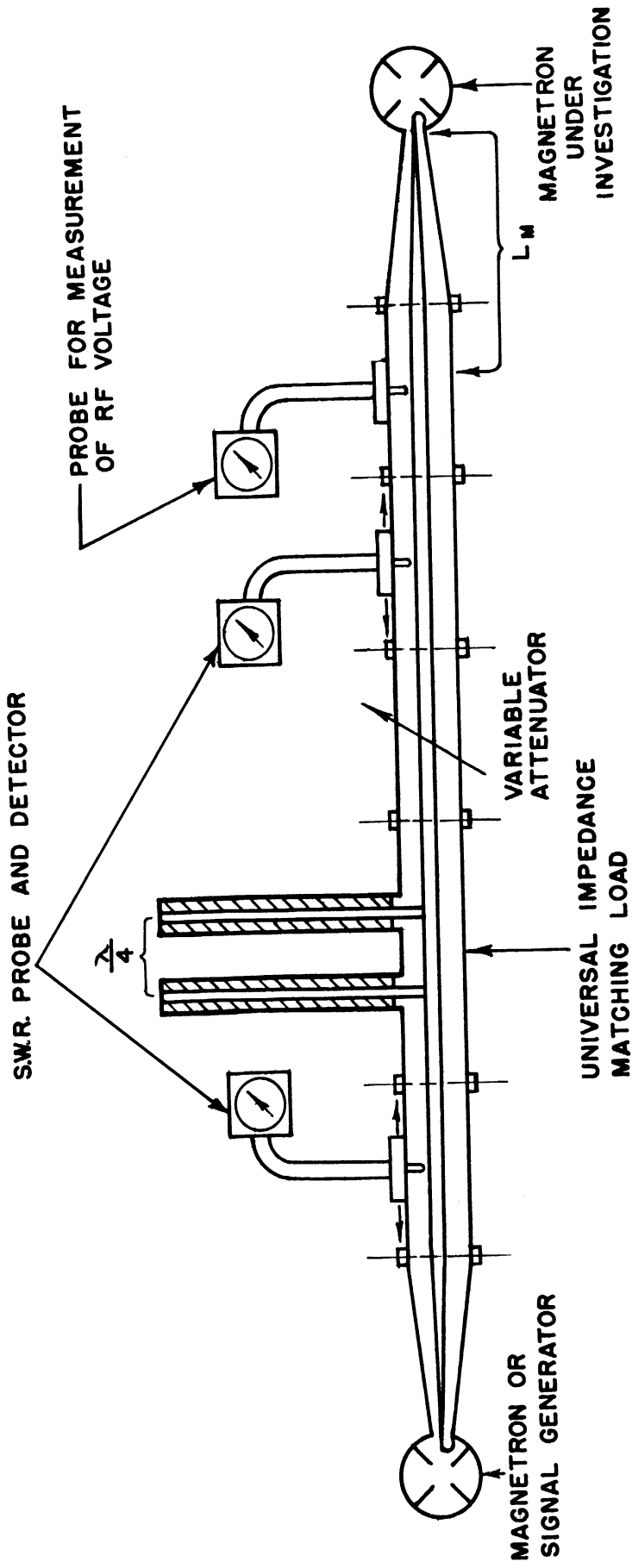


FIG. 5 EXPERIMENTAL APPARATUS FOR HOT IMPEDANCE TESTING

reverses but the original, cold-resonant wavelength is not reached. Figure 7 shows the variation of Q_0 , G_0 and λ_0 with plate voltage for different values of r-f voltages. Magnetic field is set so that oscillation begins at about 900 volts. Figure 8 shows the variation of Q_0 , G_0 and λ_0 with r-f voltage at constant plate voltage. There is a significant drop in Q_0 with increasing r-f voltage. These measurements were all recorded on the same magnetron without changing the tuner setting. The magnetron used in these tests was a QK59, a 100 watt c-w magnetron.

In Figure 9, the variation of λ_0 and G_0 with anode voltage is plotted for a low r-f voltage. Two values of magnetic field are used. In one case the value is too low to support oscillation (Figure 9a) and in the other case the value is high enough to permit oscillation (Figure 9b). Q_0 was not calculated in this case, but its behavior could be predicted roughly from the behavior of G_0 . For this magnetron, under the conditions of Figure 9b, the observed percentage change in resonant wavelength is much larger than the change observed in the data obtained on the QK59. The magnetron used was a 500 watt c-w finger magnetron designed and constructed at the University of Michigan. The cold Q_0 for this magnetron is about 500 at the point in the tuning range where these measurements were taken.

For a given frequency there exists a particular value of magnetic field for which the individual electron in the magnetron space charge will execute oscillation in phase with the r-f voltage which is impressed. This is usually called the cyclotron resonance. The sum total effect on frequency of all the individual electrons behaving in this manner can be quite large. The curves λ_0 and G_0 in Figure 10 are data taken on the same tube used for obtaining the data in Figure 9. In the course of these

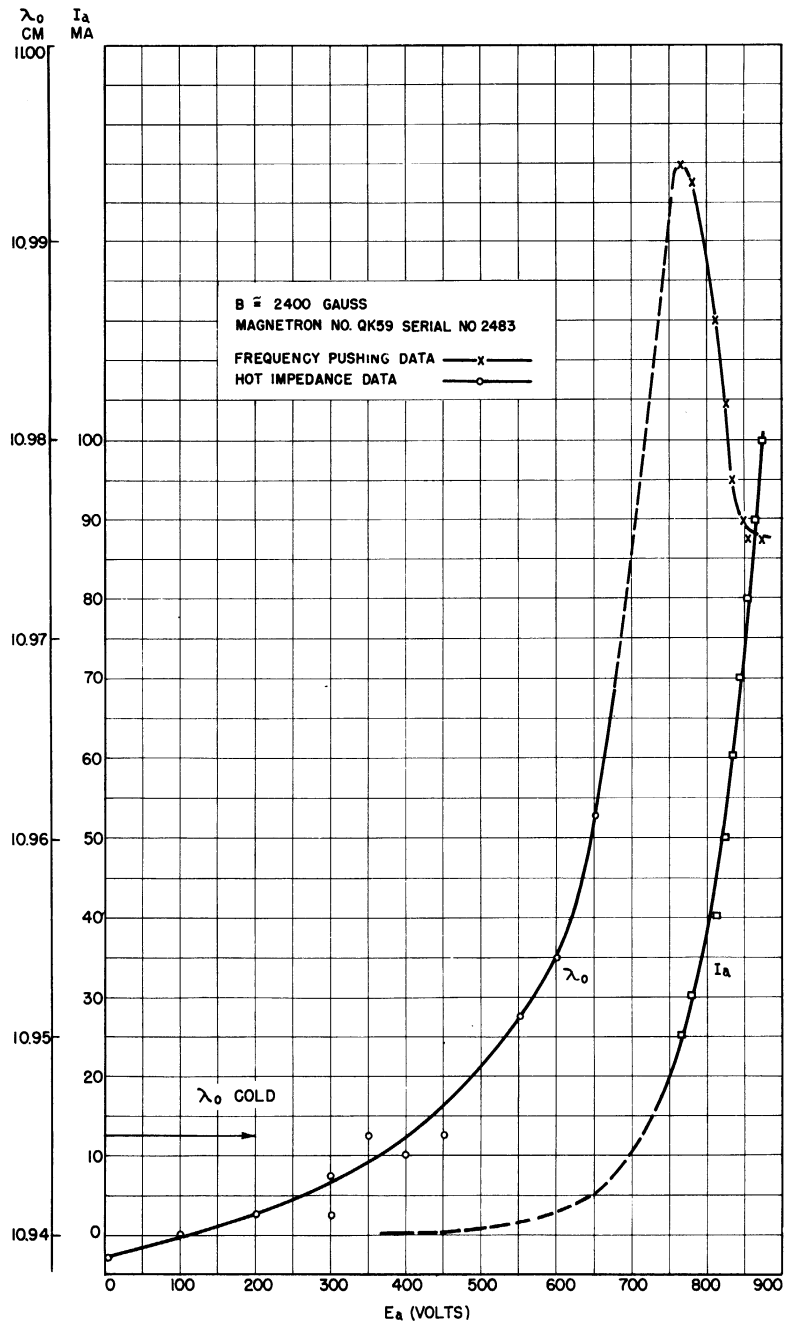


FIG. 6 CHANGE OF MAGNETRON RESONANT WAVELENGTH WITH PLATE VOLTAGE

COMPARISON OF FREQUENCY PUSHING AND HOT IMPEDANCE TEST RESULTS

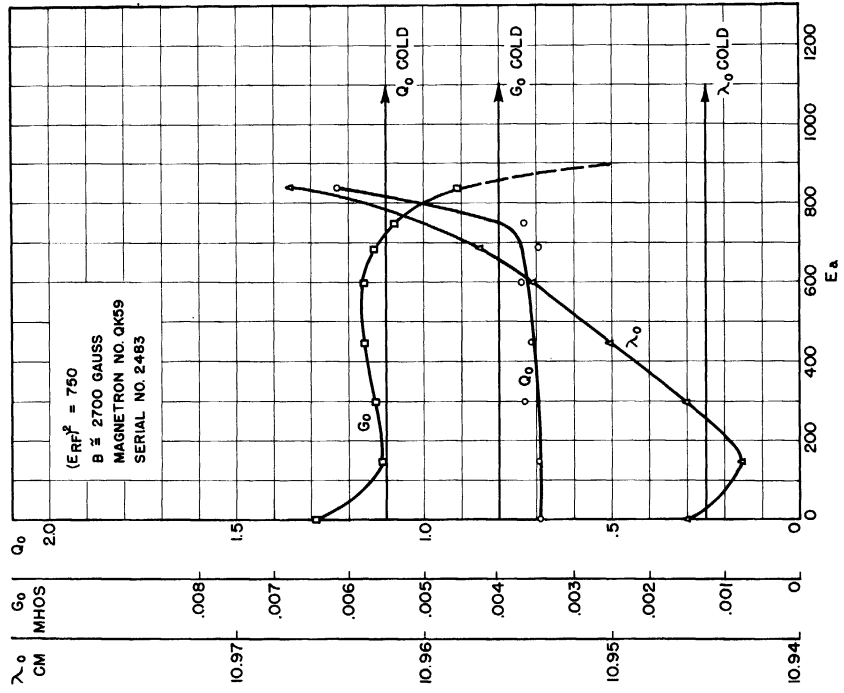


FIG. 7b

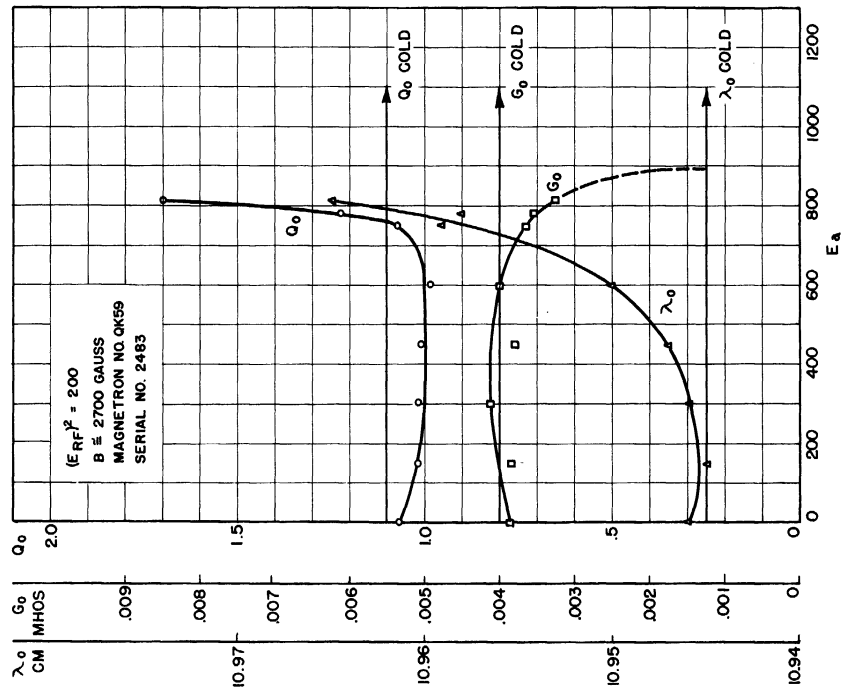


FIG. 7a

FIG. 7 Q_0, λ_0, G_0 OF HOT MAGNETRON AS A FUNCTION OF PLATE VOLTAGE FOR VARIOUS RF VOLTAGES

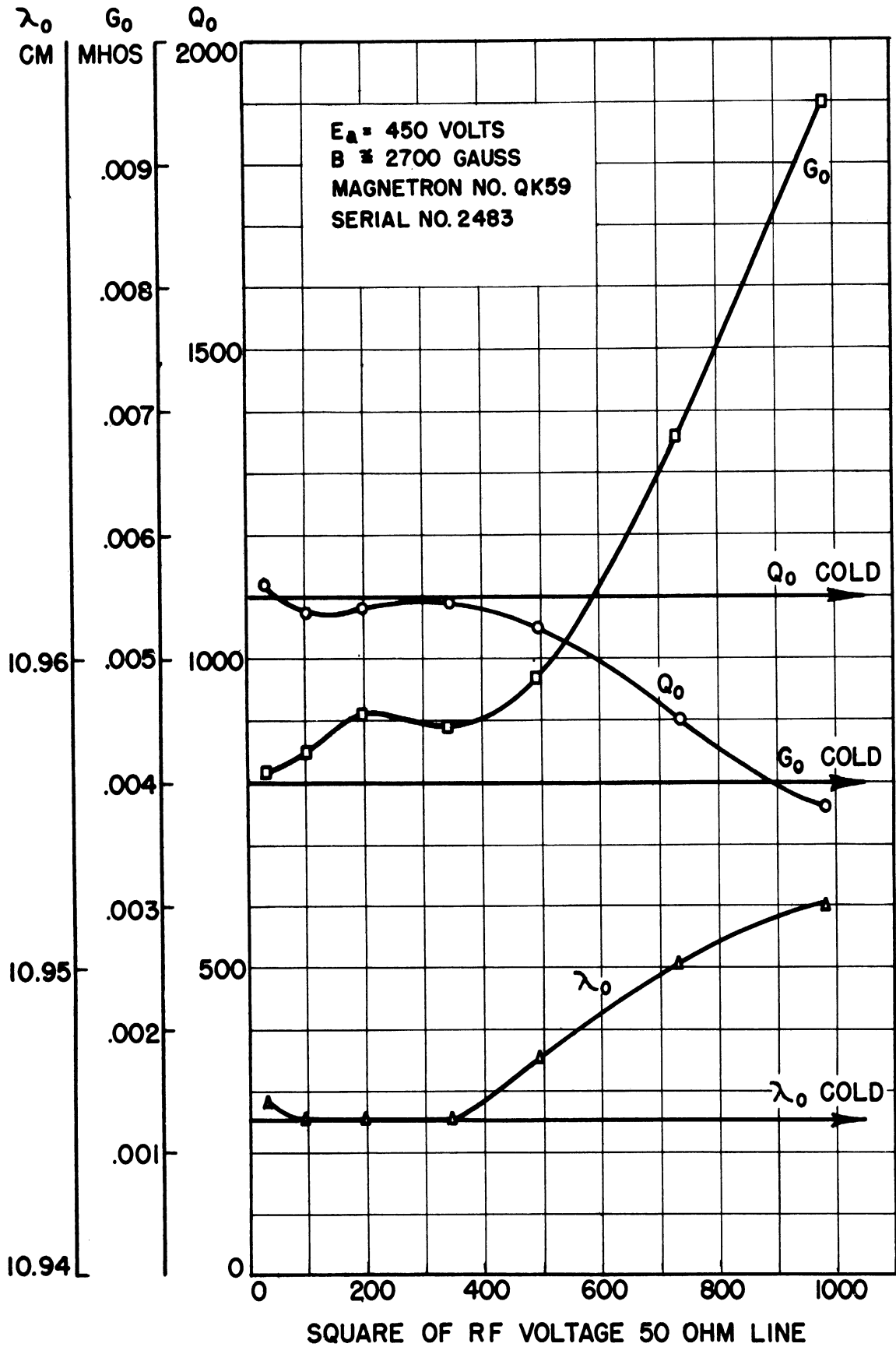


FIG. 8 Q_0, λ_0, G_0 OF HOT MAGNETRON AS FUNCTION OF RF VOLTAGE FOR PLATE VOLTAGE

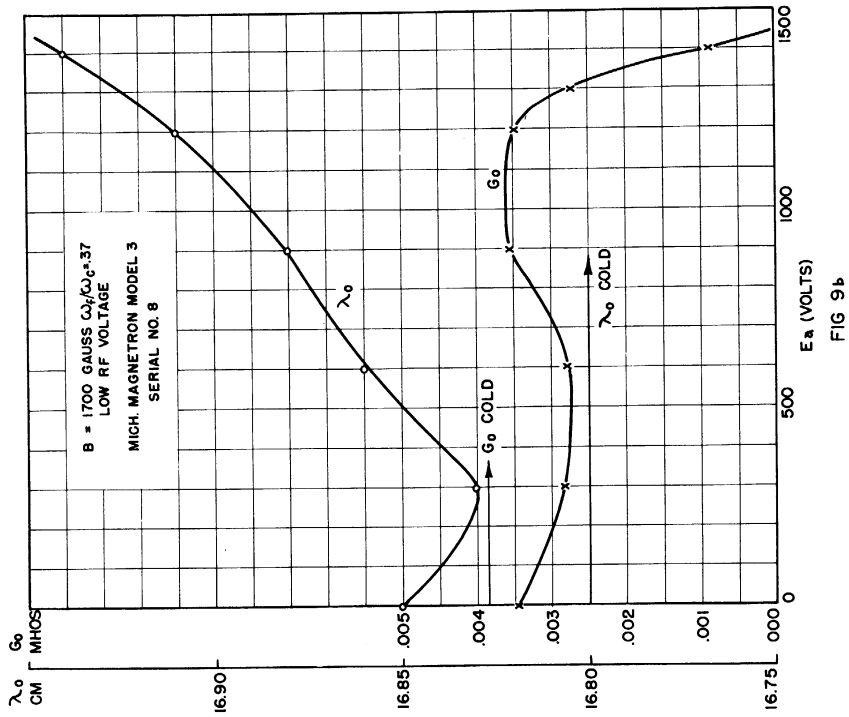


FIG 9 b

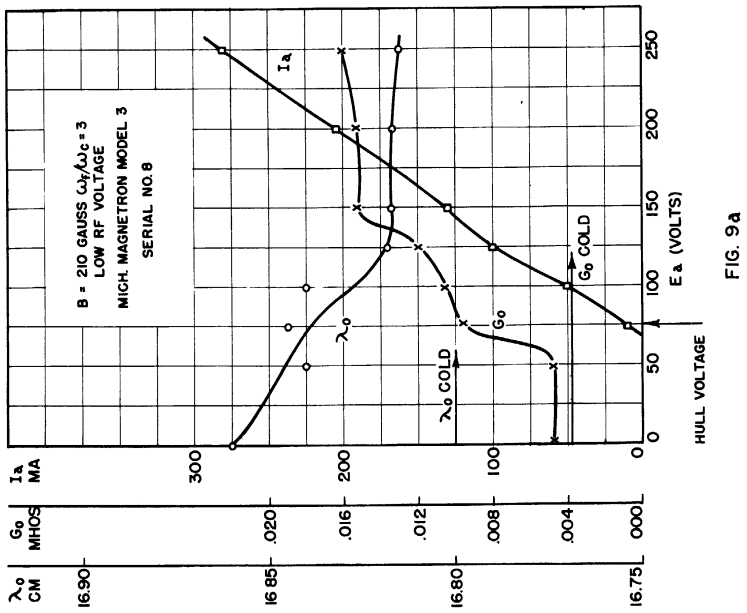


FIG. 9 a

FIG. 9 λ_0 AND G_0 OF HOT MAGNETRON AS FUNCTION OF PLATE VOLTAGE

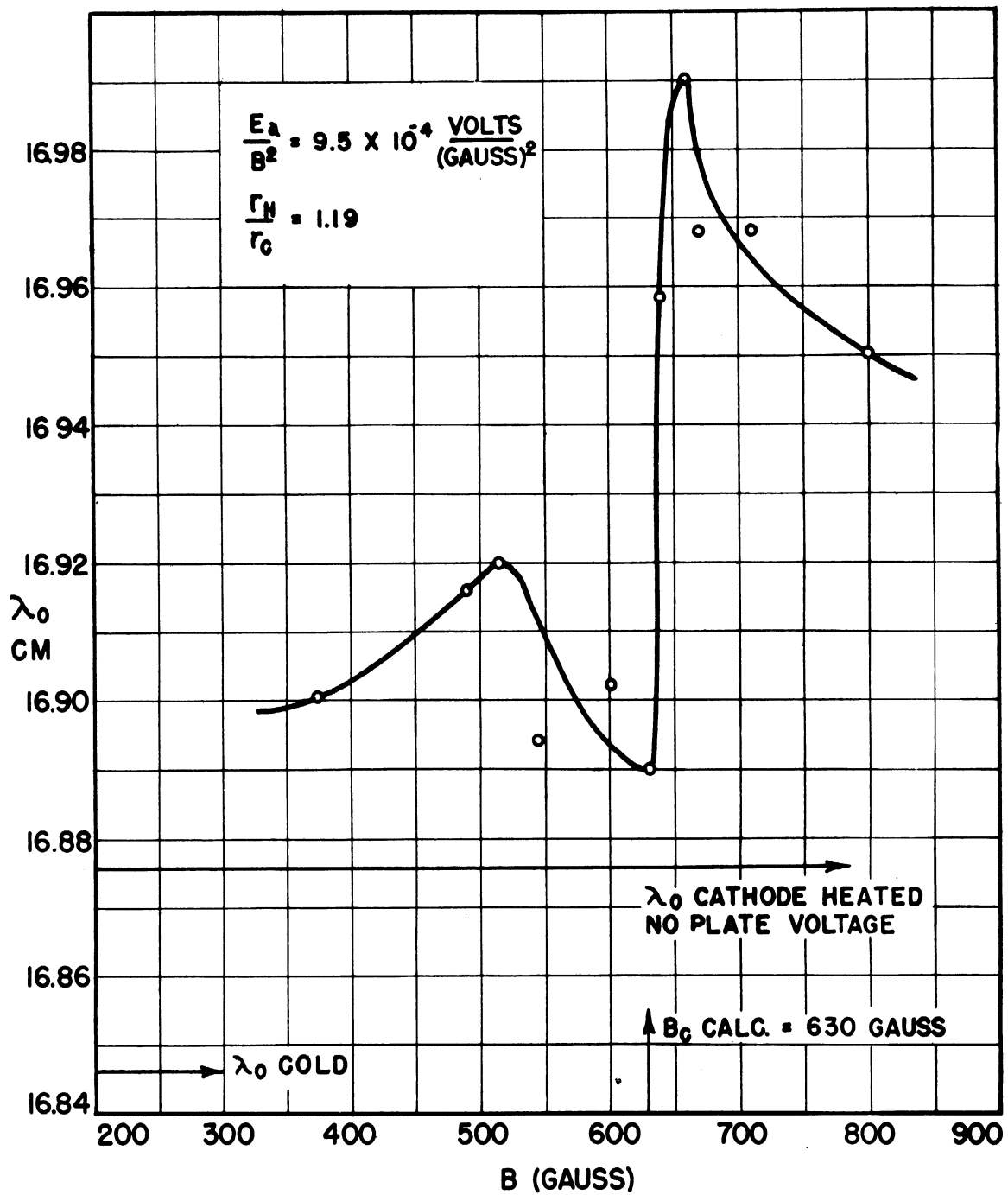


FIG. 10 DATA ON CYCLOTRON RESONANCE. λ_0 AS A FUNCTION OF MAGNETIC FIELD FOR HOT MAGNETRON. RADIUS OF SPACE CHARGE BOUNDARY CONSTANT.

measurements, the radius of the space-charge cloud was kept constant by keeping the ratio of the anode voltage to the square of the magnetic field constant (see Equation 5.13). This was done to eliminate effects of varying cloud radius on frequency. The shift of the whole resonance from the value indicated for λ_0 , no plate voltage, is due to this effect. It is interesting to observe that the maximum frequency shift is about the same as that obtained by varying voltage in the case illustrated in Figure 9.

In conclusion to this section, the relationship of the several experimental facts which are known to the problems of analysis of space-charge behavior and the development of frequency-modulation methods may be summarized:

1. A careful experimental analysis of the deviation of constant-frequency contours from the constant-susceptance lines in the Rieke diagram should yield quantitative data on the relationship of the space-charge susceptance to the space-charge conductance under given conditions of r-f voltage. In turn, a better general understanding of space-charge behavior could result.
2. Frequency pulling, a well known and comparatively well understood phenomenon, might be utilized to obtain frequency modulation. A method would have to be devised to compensate for the accompanying amplitude modulation which, in general, would result.
3. The usefulness of frequency pushing in a modulation device is doubtful. However, the data are easily and accurately taken. A theoretical analysis which could fit the experimental

results would certainly present a clearer picture of the mechanism of oscillation than we now have.

4. The data shown in Figures 6, 7, 8 and 9 indicate that frequency modulation might be obtainable by utilizing the reactive effect of a space-charge cloud controlled by conditions of voltage and magnetic field. This reactive effect might be coupled into a magnetron or other microwave device in a variety of ways which will be suggested later in this report.

5. Analysis of data of the type given in Figures 6, 7, 8 and 9 will give a picture of space-charge behavior in the pre-oscillating stage of magnetron operation.

6. The natural resonance of the electrons (Figure 10) is known to be usable in frequency modulation devices⁽¹⁾. The fact that the resonance is very sharp and has non-linearities makes its use undesirable. In modulation devices of the electron-beam type it is essential to use this resonance to have an appreciable effect on frequency. With the relatively much higher densities available in the magnetron-type rotating space charge it should be possible to avoid the use of the cyclotron resonance. An understanding of the theory of the resonance is desirable but not necessarily intimately involved with the theory of magnetron operation.

A rather important set of experimental data which has not been mentioned is that which is available on the noise output of magnetrons.

(1) VIII-2.

This work is being carried on by several groups and the results should lead to a better understanding of magnetron operation as well as, we hope, a reduction of inherent noise level⁽¹⁾. With this exception the summary indicates more or less the state of the experimental progress on this subject. In the next three sections an attempt will be made to present a picture of the space-charge behavior which fits the experimental evidence.

4. SPACE CHARGE AND THE EQUIVALENT CIRCUIT⁽²⁾

No analysis has been presented to date which gives a completely satisfactory picture of magnetron space-charge behavior. However, as one examines the many mathematical treatments and the results of experiments, a physical picture begins to form which makes more complete understanding possible where the mathematical analysis is impractical. The physical picture of the rotating space-charge cloud with spokes is commonly discussed in the description of the mechanism causing magnetron oscillation. In the case of a static magnetron, the cloud behavior is fairly well understood. The spokes, which are formed by the presence of r-f voltage, are not present and boundary conditions are more easily established. However, the non-oscillating magnetron to which is applied an r-f voltage from an external source presents a new picture. Formation of spokes is possible, but oscillation does not occur until a given voltage is reached. These conditions apply in the hot impedance tests described briefly in the last section of this report. The presence of the r-f voltages alters

(1) X-1; X-2.

(2) I-6, ch. 7.

the shape of the cloud and thus also, the reactive effect which the cloud has on the circuit. A fundamental difference between the oscillating magnetron and the non-oscillating magnetron with r-f voltage externally applied can be pointed out with reference to Figure 2.

In the case of the non-oscillating tube, an r-f voltage may be considered applied across the capacitive portion of the magnetron circuit, at the boundary between the resonant circuit structure and the interaction space. This is represented by A-A' in Figure 2a. The r-f voltage causes a current, i_T , to flow into the tank circuit. If there are electrons present in the interaction space they may be represented by an admittance, y_e , through which a current, i_e , will flow. The currents i_e and i_T are independent of each other if the r-f voltage is assumed unaffected by their magnitudes. If the admittance of the tank circuit is known the admittance, y_e , could presumably be measured. This admittance should be dependent upon the values of magnetic field, anode voltage, r-f voltage and geometry of the interaction space.

The circuit of the oscillating magnetron is represented in Figure 2b. In this case the current i_T , developed in the tank circuit, is induced by the cloud of electrons rotating in the interaction space. This current results in an r-f voltage at the terminals A-A'. The current cannot exist until the oscillations become regenerative. The spokes on the space-charge cloud cannot exist until r-f voltages are present, i.e., until oscillation starts. The rotating cloud with spokes may be thought of as a current generator. There is a phase difference between the generated current and the r-f voltage which causes the oscillations to build up at a lower frequency than the natural resonance frequency of the tank circuit. This phase difference and the equivalent negative conductance of

the electrons are represented in y_e , the admittance equivalent to the generator representing the electrons. The value of this admittance must be such that the net susceptance and conductance of the circuit are cancelled at the frequency of oscillation. When the admittance characteristic of the tank circuit is known as a function of frequency near resonance, the value of y_e can be calculated.

These two interpretations of y_e should be kept in mind while reading the following sections. We will find that in the first case for the non-oscillating magnetron the space-charge effects on frequency are primarily a function of the dimensions and density of the hub of the space-charge wheel. In the second case of the oscillating magnetron the effect on frequency is due to the phase relation of the spokes to the r-f voltage. The two effects cause frequency shifts in opposite directions. In the first case, quantitative agreement between experiment and theory is shown. In the second case only qualitative discussion is thus far possible.

5. ANALYSIS OF SPACE-CHARGE BEHAVIOR

The mathematical analysis of space-charge behavior is based on the force equation for an electron in an electromagnetic field. This equation in vector form is the following

$$\frac{d\vec{v}}{dt} = - \frac{e}{m} (\vec{F} + \vec{v} \times \vec{B}) \quad (5.1)$$

where

e = absolute value of electronic charge

m = mass of electron

\vec{v} = velocity of electron

\vec{F} = vector value of electric field

\vec{B} = vector value of magnetic field

The magnetron will be considered with axial alignment in the z-direction. In this case it is convenient to resolve the vector quantities in Equation 5.1 into components in cylindrical coordinates. If proper account is taken of the symmetries in the magnetron, Equation 5.1 may be written as follows:

$$\begin{aligned} \frac{d\vec{v}}{dt} &= \vec{r}_1 \left\{ \frac{dv_r}{dt} - r\omega^2 \right\} + \vec{\theta}_1 \left\{ 2v_r\omega + r \frac{d\omega}{dt} \right\} \quad (5.1a) \\ &= -\frac{e}{m} (\vec{r}_1 F_r + \vec{\theta}_1 F_\theta + \vec{r}_1 r\omega B_z - \vec{\theta}_1 v_r B_z) \end{aligned}$$

Here the quantities with subscript (1) are unit vectors. \vec{v} has been replaced by

$$\vec{v} = \vec{r}_1 v_r + \vec{\theta}_1 r\omega \quad (5.2)$$

$r\omega$ is therefore the magnitude of the θ -directed component of velocity. ω is the angular velocity of the electron. The components F_z , v_z , B_θ , B_r are considered non-existent as would be the case in an ideal magnetron. By separation of the r- and θ -directed components in Equation 5.1a we obtain the following two important equations for scalar quantities.

$$\boxed{\frac{dv_r}{dt} - r\omega^2 = -\frac{e}{m} (F_r + r\omega B_z)} \quad (5.3a)$$

$$\boxed{2v_r\omega + r \frac{d\omega}{dt} = -\frac{e}{m} (F_\theta - v_r B_z)} \quad (5.3b)$$

There are several results to be derived from these two equations based on various assumptions which may be used. We will consider two cases of interest. Since B is always in the z-direction we will drop the subscript z.

Case I - The Non-Oscillating Magnetron, No R-F Voltage Present

We will first assume that no r-f field is present; therefore,

$F_{\theta} = 0$. In this case Equation 5.3b can be written:

$$2 \frac{dr}{dt} (\omega_L - \omega) = r \frac{d\omega}{dt} \quad (5.4)$$

v_r has been replaced by $\frac{dr}{dt}$ and $\frac{e B}{m \omega}$ has been replaced by ω_L . Separating variables we have

$$\frac{2dr}{r} = - \frac{d\omega}{\omega - \omega_L}$$

This equation has the general solution:

$$\log_e r^2 = - \log_e (\omega - \omega_L) + \log c$$

or

$$r^2 = \frac{c}{\omega - \omega_L}$$

At the boundary of the cathode r_c , ω is assumed to be zero. Therefore,

$$c = -\omega_L r_c^2$$

and we have finally, for the angular velocity of an electron at radius r under static conditions

$$\boxed{\omega = \omega_L \left(1 - \frac{r_c^2}{r^2}\right)} \quad (5.5)$$

This value of ω may be substituted back into Equation 5.3a, yielding

$$\frac{dv_r}{dt} - r\omega_L^2 \left(1 - \frac{r_c^2}{r^2}\right)^2 = - \frac{e}{m} F - 2r\omega_L^2 \left(1 - \frac{r_c^2}{r^2}\right) \quad (5.6)$$

$$\frac{dv_r}{dt} = \frac{\partial v_r}{\partial t} + \frac{\partial v_r}{\partial r} v_r$$

If a steady state condition is assumed, i.e., v_r does not change with time

$$\frac{\partial v_r}{\partial t} = 0$$

F_r may be rewritten in terms of the potential E .

$$F_r = - \frac{\partial E}{\partial r}$$

If we make the additional simplifying assumption that $v_r = 0$, i.e., no radial current, Equation 5.6 becomes

$$F_r = - \frac{\partial E}{\partial r} = \frac{m}{e} r \omega_L^2 \left(\frac{r_c^4}{r^4} - 1 \right) \quad (5.7)$$

This may be substituted in Poisson's equation to determine the space-charge density, ρ .

$$\frac{\rho}{\epsilon_0} = - \frac{1}{r} \frac{\partial}{\partial r} \left(r \frac{\partial E}{\partial r} \right)$$

or

$$\frac{\rho}{\epsilon_0} = - 2 \frac{m}{e} \omega_L^2 \left[1 + \left(\frac{r_c}{r} \right)^4 \right] \quad (5.8)$$

ϵ_0 = dielectric constant of free space = $1/36 \pi \times 10^{-9}$ farads/m

The potential distribution is obtained by integrating Equation 5.7. If E_c is the potential at the cathode and E the potential at r then

$$E - E_c = - \frac{m}{e} \omega_L^2 \int_{r_c}^r \left(\frac{r_c^4}{r^3} - r \right) dr$$

Integrating and substituting the limits we obtain

$$E - E_c = \frac{m}{2e} \omega_L^2 r^2 \left(1 - \frac{r_c^2}{r^2} \right)^2 \quad (5.9)$$

This represents theoretically a voltage above which electrons must be found at a radius r in the static magnetron. If this equation is satisfied all of the energy extracted by the electrons from the electric field has been converted into kinetic energy of motion in the angular direction. The electrons are, in this case, traveling in stable orbits around the cathode with an angular velocity as given by Equation 5.5. The radial velocity is zero everywhere. This distribution does not explain any transient conditions, or conditions in which there is a net radial current. It

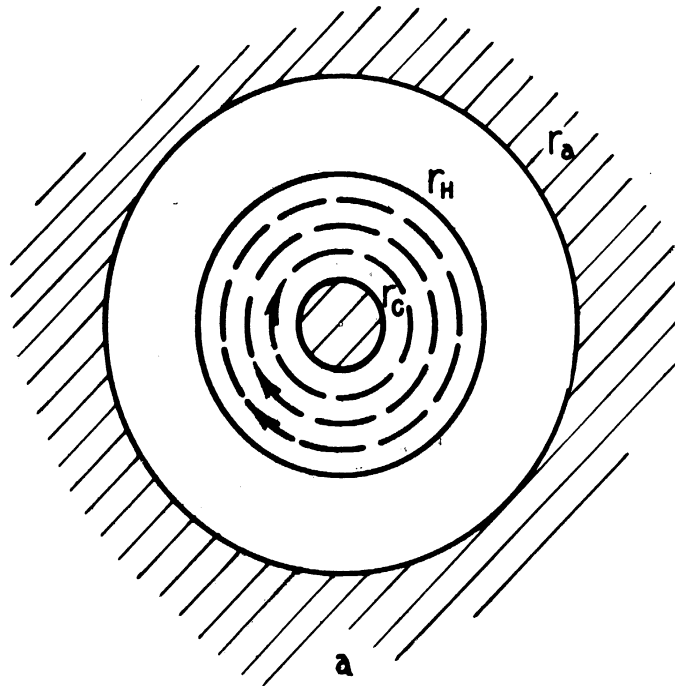
describes a potential distribution and space-charge distribution which conceivably might exist in a static magnetron.

The Equation 5.5 for the angular velocity of the electrons as a function of radius is more general than the equation for the potential distribution. The following assumptions are sufficient to arrive at this conclusion: (a) the θ component of the field is zero; (b) there is no energy exchange with the surroundings. No restrictions are placed on the radial velocity. If conditions a and b are met, an electron at a given radius must have the angular velocity given by Equation 5.5. Under these conditions the potential distribution, 5.9, is fulfilled at the outer edge of the space-charge cloud, regardless of the conditions placed on radial velocity within the cloud. If there is energy exchange causing the electron angular velocity to be changed from the value given by Equation 5.5, the Equation 5.9 for the potential distribution no longer holds true.

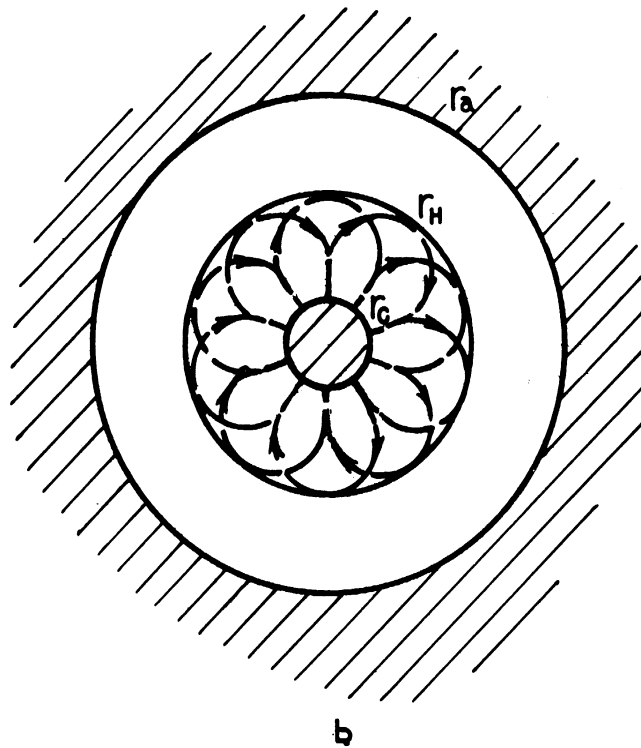
If we assume that the distribution of voltage of Equation 5.9 does exist within a static magnetron drawing no anode current, another interesting formula may be derived. This will show how anode voltage and radius of the space-charge cloud are related.

The charge per unit length in a cylindrical magnetron may be found by integrating the space-charge density of Equation 5.8. Referring to Figure 11a, and defining r_H as the maximum radius at which space charge is found in the cloud, we may write for the total space charge per unit length within this cloud:

$$\tau = - \int_{r_c}^{r_H} 2\pi \epsilon_0 \frac{2m}{e} \omega_L^2 \left(r + \frac{r_c^4}{r^3} \right) dr$$



SINGLE STREAM CIRCULAR TRAJECTORIES



DOUBLE STREAM TRAJECTORIES WITH RADIAL VELOCITIES

FIG. II HYPOTHETICAL ELECTRON PATHS WITHIN
MAGNETRON SPACE CHARGE.

Evaluating this integral

$$\tau = -2\pi \epsilon_0 \frac{m}{e} \omega_L^2 r_H^2 \left(1 - \frac{r_c^4}{r_H^4}\right) \quad (5.10)$$

For a cylindrical diode

$$E_a - E' = -\frac{\tau}{2\pi \epsilon_0} \log \frac{r_a}{r'} \quad (5.11)$$

E_a is the anode voltage, E' is a voltage at some point in charge free space. If we let $E' = E_H$, and $r' = r_H$ where E_H is at the boundary of the Hull space-charge cloud, r_H , we have

$$E_a - E_H = \frac{m}{e} \omega_L^2 r_H^2 \left(1 - \frac{r_c^4}{r_H^4}\right) \log \frac{r_a}{r_H} \quad (5.12)$$

Obtaining an expression for E_H from Equation 5.9, by letting $E_c = 0$ and replacing ω_L by $\frac{Be}{2m}$, we have finally

$$E_a = B^2 \frac{e}{8m} r_H^2 \left[2\left(1 - \frac{r_c^4}{r_H^4}\right) \log \frac{r_a}{r_H} + \left(1 - \frac{r_c^2}{r_H^2}\right)^2 \right] \quad (5.13)$$

This equation shows us that, for a given magnetron, if E_a/B^2 is kept constant, the radius of a space-charge cloud remains constant. Also, if r_H is allowed to equal r_a , the anode radius, we have the Hull cutoff equation, the condition for which electrons must reach the anode.

It should be emphasized that Equation 5.13 no longer holds true if the space-charge distribution is other than that given by Equation 5.8. This may be the case even when the voltage at the edge of the cloud is given by Equation 5.9, as it must be if there is no radial velocity at the edge of the cloud and no energy exchange with the surroundings. Reference to Figure 11 will make this point clear. In Figure 11a, the situation described by Equation 5.13 is represented. Here the electrons travel in circles, represented by the dotted lines, around the cathode. The voltage

distribution within r_H is given by Equation 5.9 and outside r_H by Equation 5.12. r_H has the value determined from Equation 5.13 for the given anode voltage E_a . In Figure 11b, another situation is pictured in which the voltage at r_H would still be given by Equation 5.9. In this case, the electrons leave the cathode with zero velocity and gain velocity, both radial and tangential, as they go outward until the point r_H is reached. At this point, the velocity is all tangential. The electron then gives up this kinetic energy of velocity, returning to the cathode and arriving with zero velocity. A new voltage distribution must exist within the cloud. This follows from the fact that the distribution of angular velocity remains the same in satisfaction of Equation 5.3b, whereas there is also present a radial velocity. The added kinetic energy of radial motion must be due to the electron experiencing a potential drop greater than that given by the distribution, 5.9. This relationship can, therefore, no longer be true within the cloud and the space-charge distribution used in derivation of Equation 5.13 can no longer be correct.

Solutions for trajectories of the type pictured in Figure 11b have been obtained. Attempts to calculate the space-charge and potential distribution have not been successful. The boundary conditions are much less restricting than those used in the case discussed here. The radial acceleration is assumed to be zero only at the cathode and the radial velocity is assumed to be zero at the outer boundary of the space charge. Within the space charge v_r is unrestricted by the initial assumptions. There should be an infinite number of solutions which satisfy these conditions. It has been shown that the multiple stream solution is only possible for values of $r_a/r_c > 2.271$. Even then it possibly exists only in the transitory state⁽¹⁾. Most c-w magnetrons have values of $r_a/r_c < 2.271$. We

(1) V-5.

will show in discussing the experimental results that the single stream solution which has been presented here is sufficiently accurate to describe most types of behavior. It is in the transference from the condition of the non-oscillating magnetron to the oscillating magnetron that the mathematical development is insufficient. In Case II which follows we will discuss a condition of the space charge which could possibly exist in a magnetron just beginning to oscillate.

Case II - Non-Oscillating Magnetron with R-F Voltage Applied
From External Source

The second case of interest is one which is artificial and probably not existent in a self-excited magnetron. An understanding of this case, however, is very useful background for discussion of the oscillating magnetron. The effect of magnitude of the r-f voltage can only be speculated upon the basis of the theory presented here. It is interesting to note that the method of calculating the voltage at which the magnetron starts to oscillate (the Hartree voltage) does not depend upon any assumptions as to this magnitude.

It will be convenient to define some terms which will simplify the following discussion and will make the terminology the same as that generally used in discussing the scaling of magnetrons⁽¹⁾. These definitions also have the advantage of making most of the equations dimensionless. The presence of the r-f is described in the usual manner⁽²⁾. The r-f wave with which the electrons interact is considered as traveling around the interaction space between anode and cathode, with an angular velocity given by

(1) I-4.

(2) I-3.

$$\omega_n = \frac{2\pi f}{n} \quad (5.14)$$

f is the frequency of the r-f impressed on the magnetron anodes.
 n is the mode number, equal to $N/2$ in the π mode where N is
the number of anodes.

The kinetic energy of an electron at the anode having the angular velocity given by Equation 5.14 defines a voltage which we will call E_0

$$E_0 = \frac{m}{2e} \omega_n^2 r_a^2 \quad (5.15)$$

The magnetic field which would allow this angular velocity to exist at the anode of a non-oscillating magnetron is defined by Equation 5.5 when ω is equal to ω_n and r set equal to r_a

$$B_0 = \frac{2m}{e} \omega_n \left[\frac{1}{1 - \frac{r_c^2}{r_a^2}} \right] \quad (5.16)$$

In terms of these variables the Equation 5.9 may be written

$$\frac{E - E_c}{E_0} = \left(\frac{B}{B_0} \right)^2 \quad (5.9a)$$

E_0 and B_0 depend only on dimensions of the magnetron, the frequency impressed on the magnetron anodes and physical constants.

Let us first assume that the Hull distribution 5.9 exists within the magnetron and that an r-f voltage impressed upon the anodes causes a perturbation of this distribution. As the voltage is raised the cloud will become larger and the angular velocity will increase according to Equation 5.5. As long as the angular velocity of the electrons is less than the angular velocity of the traveling wave there can be no energy transferred from the electron cloud to the r-f field. The electrons, however, can take energy from the r-f. The increase in velocity so obtained would cause an increase in force due to the motion in a magnetic field

which would not be balanced by the simultaneous increase in centrifugal force. The energy acquired by these electrons would be expended in the cathode.

At a particular voltage, outer electrons in the swarm reach the angular velocity of the r-f field. Above this voltage the outer electrons are trying to travel faster than the field. This excess energy will be absorbed by the r-f field until the electrons are slowed to the synchronous velocity. During this process of energy absorption the electrons will drift outward from the edge of the swarm. The potential distribution outside the swarm will thus be altered by the presence of the space charge.

In order to get an idea of the radius of the space charge for which synchronism takes place, it is convenient to rewrite Equation 5.13 in terms of the new variables as follows:

$$\frac{E_a}{E_0} = \left(\frac{B}{B_0}\right)^2 \left(\frac{r_H}{r_a}\right)^2 \left[\frac{\left(1 - \frac{r_c^4}{r_H^4}\right)}{\left(1 - \frac{r_c^2}{r_a^2}\right)^2} \log \frac{r_a}{r_H} + \left(\frac{1 - \frac{r_c^2}{r_H^2}}{1 - \frac{r_c^2}{r_a^2}}\right)^2 \right] \quad (5.13a)$$

Using the definition of B_0 we may write

$$\frac{\omega}{\omega_n} = \frac{B}{B_0} \frac{1 - \frac{r_c^2}{r^2}}{1 - \frac{r_c^2}{r_a^2}} \quad (5.17)$$

When $\omega = \omega_n$

$$\frac{B_n}{B_0} = \frac{1 - \frac{r_c^2}{r_a^2}}{1 - \frac{r_c^2}{r_n^2}} \quad (5.18)$$

The subscript n denotes values for which the angular velocity of the outer edge of the electron swarm reaches synchronism with the angular velocity of the wave. The voltage for which synchronism occurs at a given radius is given by substitution of B/B_0 from Equation 5.18 into Equation 5.13a. We are discussing the outer edge of the cloud so $r_H = r_n$.

$$\frac{E_{an}}{E_0} = \frac{r_n^2}{r_a^2} \left[2 \frac{1 + \frac{r_c^2}{r_n^2}}{1 - \frac{r_c^2}{r_n^2}} \log \frac{r_a}{r_n} + 1 \right] \quad (5.19)$$

An interesting conclusion to be drawn from these equations (5.18 and 5.19) is that for given values of ω_n and r_n and a given tube geometry there is only one set of values for E_a/E_0 and B/B_0 , which will allow the edge of the electron swarm to rotate in synchronism.

By eliminating r_n between these two equations, we may write an equation relating E_a/E_0 and B/B_0 for the condition that the outermost electrons in the cloud have just reached synchronism.

$$\frac{E_{an}}{E_0} = \frac{B_n}{B_0} \frac{\frac{r_c^2}{r_a^2}}{\frac{B_n}{B_0} - (1 - \frac{r_c^2}{r_a^2})} \left[2 \left(\frac{B_n}{B_0} \frac{2}{1 - \frac{r_c^2}{r_a^2}} - 1 \right) \log \frac{\sqrt{\frac{B_n}{B_0} - (1 - \frac{r_c^2}{r_a^2})}}{\frac{r_c}{r_a} \sqrt{\frac{B_n}{B_0}}} + 1 \right] \quad (5.20)$$

Let us now examine the potential distribution in a region where electrons are in synchronism. This can be derived quite simply from the original force equation if we make the initial assumption that the angular velocity of the electrons is the synchronous velocity ω_n . In this case, Equation 5.3a is written

$$\frac{dv_r}{dt} - r\omega_n^2 = -\frac{e}{m} (F_r + r\omega_n B_z)$$

We assume as we did before steady state with no radial acceleration; i.e., all energy is kinetic energy of rotation. In this case it will be convenient to make the substitution:

$$\omega_c = \frac{Be}{m} = 2\omega_L \quad (5.21)$$

We have therefore

$$F_r = -\frac{\partial E}{\partial r} = \frac{m}{e} r\omega_n (\omega_n - \omega_c) \quad (5.22)$$

This equation can be rewritten

$$-\frac{\partial}{\partial r} \left(\frac{E}{E_0} \right) = 2 \frac{r}{r_a^2} \left(1 - \frac{\omega_c}{\omega_n} \right)$$

Integrating this becomes:

$$-\frac{E}{E_0} = \left(1 - \frac{\omega_c}{\omega_n} \right) \frac{r^2}{r_a^2} + C \quad (5.23)$$

In order to evaluate C we will make use of the assumption that all energy is kinetic energy of angular velocity. Thus at the boundary $r = r_n$

$$eE_n = \frac{m}{2} \omega_n^2 r_n^2$$

and at the anode

$$eE_0 = \frac{m}{2} \omega_n^2 r_a^2$$

Therefore, dividing one equation by the other, we have at $r = r_n$

$$\frac{E_n}{E_0} = \frac{r_n^2}{r_a^2} \quad (5.24)$$

Using this relationship as a boundary condition to evaluate C, Equation 5.23 becomes

$$\frac{E}{E_0} = -\frac{r^2}{r_a^2} + 2\frac{r_n^2}{r_a^2} + \frac{\omega_c}{\omega_n} \left(\frac{r^2}{r_a^2} - \frac{r_n^2}{r_a^2} \right) \quad (5.25)$$

There are two ways of expressing ω_c/ω_n which are useful in simplifying Equation 5.25. These are

$$\frac{\omega_c}{\omega_n} = 2\frac{B}{B_0} \frac{1}{1 - \frac{r_c^2}{r_a^2}} \quad (5.26)$$

(from the definitions of ω_c in 5.21 and B_0 in 5.16) and

$$\frac{\omega_n}{\omega_c} = \frac{1}{2} \left(1 - \frac{r_c^2}{r_n^2} \right) \quad (5.27)$$

The latter relationship is based on the assumption that the solution in Equation 5.5 holds out to r_n . Rewrite 5.25

$$\frac{E}{E_0} = \frac{\omega_c}{\omega_n} \left(\frac{r^2}{r_a^2} - \frac{r_n^2}{r_a^2} + 2\frac{r_n^2}{r_a^2} \frac{\omega_n}{\omega_c} \right) - \frac{r^2}{r_a^2}$$

If we make the substitutions 5.26 and 5.27 for the quantity ω_c/ω_n outside the bracket and inside the bracket, respectively, the result becomes

$$\boxed{\frac{E}{E_0} = 2\frac{B}{B_0} \frac{\frac{r^2}{r_a^2} - \frac{r_c^2}{r_a^2}}{1 - \frac{r_c^2}{r_a^2}} - \frac{r^2}{r_a^2}} \quad (5.28)$$

This new potential distribution exists throughout the distribution of space charge which forms outside the "Hull" cloud because of electrons being slowed to synchronism. If the outermost electrons of this cloud are just capable of reaching the anode the magnetron will draw plate current. The electrons must give up energy to reach this radius; therefore, as soon as the magnetron is capable of drawing current, it will be able to use this energy to generate oscillations. This assumes of course that ω_n corresponds to a frequency at which the magnetron

resonator will oscillate. This condition may be imposed upon Equation 5.28 and we have, for $r = r_a$

$$\boxed{\frac{E_a}{E_0} = 2 \frac{B}{B_0} - 1} \quad (5.29)$$

This is the well known Hartree equation defining the voltage at which oscillations can begin⁽¹⁾. The effect of the presence of r-f voltage is to alter the angular velocity given by 5.27. If no r-f voltage is present, Equation 5.29 should accurately define the voltage at which oscillation starts.

One other equation of some interest can be derived from these relationships. This is the equation for the space charge under the conditions of what we will henceforth call the Hartree distribution. If we apply Poisson's equation to Equation 5.22 the result is

$$\boxed{\rho = -2 \epsilon_0 \frac{m}{e} \omega_n (\omega_c - \omega_n)} \quad (5.30)$$

The space charge in the Hartree distribution is therefore a constant independent of the radius and dependent only on the angular velocity of the wave, the magnetic field and physical constants.

If the distribution in the portion of the space-charge cloud traveling at less than the synchronous velocity ω_n is presumed to be the Hull distribution, the space-charge density at the outside edge of the Hull cloud and the inside edge of the Hartree cloud are of different magnitude. Making the substitution

$$\omega_n = \omega_L \left(1 - \frac{r_c^2}{r_n^2}\right)$$

(1) V-4.

in the equation for the Hull space-charge distribution, 5.8, this equation becomes

$$\rho = -2 \epsilon_0 \frac{m}{e} \left[\frac{\omega_c^2}{2} - \omega_n (\omega_c - \omega_n) \right] \quad (5.8a)$$

at the boundary between the two distributions. Thus, at the boundary,

$$\frac{\rho_{\text{Hull}}}{\rho_{\text{Hartree}}} = \frac{1}{2} \frac{\omega_c^2}{\omega_n (\omega_c - \omega_n)} - 1 \quad (5.31)$$

Similar algebraic manipulation with the equations for the field and for the potential distribution will show that these quantities are exactly equal at the boundary between the two clouds.

In order to summarize this section we will mention the numbers of the most important equations resulting from the analysis of these two cases. The most interesting of the results are plotted in Figures 12 to 17. Study of these curves with dimensions of physical magnetrons in mind will give one an idea of typical values for the various parameters and their relationship to each other.

Case I. Non-oscillating magnetron, no r-f voltage present.

The important relationships are the following:

- Equation 5.5 for angular velocity of electrons
- 5.7 for field distribution
- 5.8 for space-charge distribution
- 5.9 and 5.9a for potential distribution
- 5.13 and 5.13a relating anode potential, magnetic field and radius of space charge

Case II. Non-oscillating magnetron, r-f voltage present.

The important relationships are the following:

- Equations 5.14, 5.15 and 5.16 defining respectively ω_n ,

E_0 and B_0

- Equation 5.18 giving magnetic field for which electrons
at given radius attain synchronous velocity
- 5.19 giving anode potential for which electrons
at given radius attain synchronous velocity
- 5.20 relating anode voltage and magnetic field
for synchronous angular velocity at edge
of Hull cloud
- 5.22 for field distribution
- 5.24 voltage at r_n for synchronism
- 5.28 for potential distribution
- 5.29 relating voltage and magnetic field for
initiation of oscillation
- 5.30 for space-charge distribution

The physical picture to be derived from this analysis and the interpretation in the light of available experimental data will be discussed following the next section. We will investigate in the next section the space charge from the point of view of its wave propagating properties.

6. PROPAGATION OF THE ELECTROMAGNETIC WAVE IN THE MAGNETRON SPACE CHARGE

In the last section we have dealt primarily with the formation of the space charge and its behavior under special conditions. In this section we will try to ascertain some of the properties of the space

charge as formed. The properties of the space-charge cloud have been analyzed previously⁽¹⁾, but points of particular interest to the problem of frequency modulation by a space-charge cloud have not been emphasized.

The space-charge cloud, for small signal strengths, can be considered in the manner that one considers a free electron gas. Large signal strengths cause enough perturbation in the electron paths to produce cathode bombardment. This has the effect of introducing a damping term in the equation of motion which is neglected in the treatment of a free electron gas. There is no significant damping effect in an atmosphere of free electrons because complete energy transfer occurs in collisions between electrons. In this sense we cannot compare the electron gas to a conductor because mean free paths are infinite; whereas, in the conductor, they are determined by the presence of large molecules. Collisional damping makes conductivity finite.

In this treatment we will assume the space charge present in the magnetron to be given by the results of the last section. Since we are considering the space charge as an atmosphere of determined density and boundary, it is immaterial what system of coordinates is used for the force equations. The force equation for an electron in the presence of an r-f field $\vec{F} = \vec{F}_0 e^{-j\omega_f t}$ is as follows:

$$\frac{d\vec{v}}{dt} = -\frac{e}{m} \vec{F}_0 e^{-j\omega_f t} \quad (6.1)$$

neglecting any damping effects. If we integrate with respect to t , the result is

$$\vec{v} = -j \frac{e}{m \omega_f} \vec{F}_0 e^{j\omega_f t}$$

(1) VI-1,3.

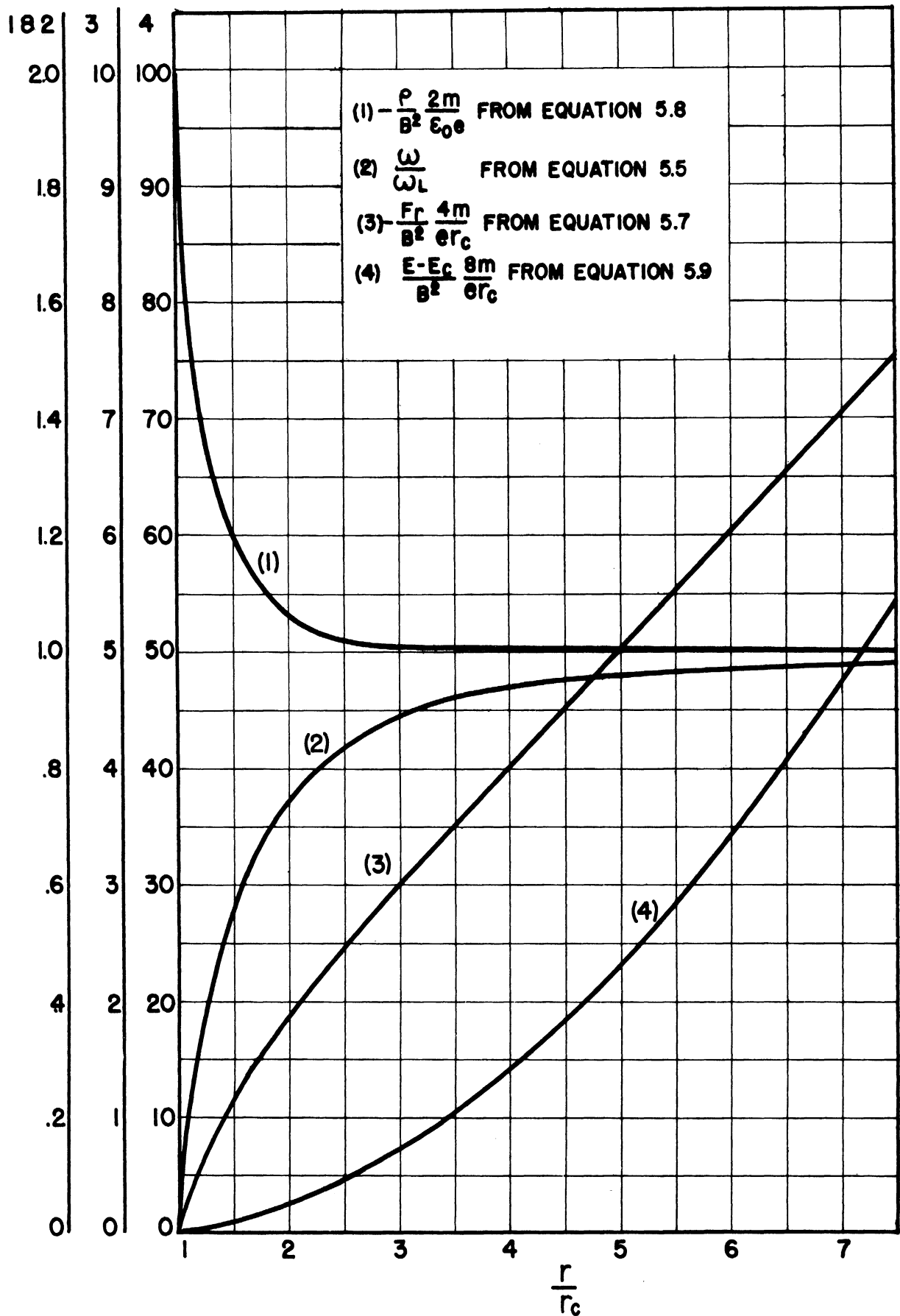


FIG. 12 CASE I. DISTRIBUTIONS EXISTING IN THE STATIC MAGNETRON.

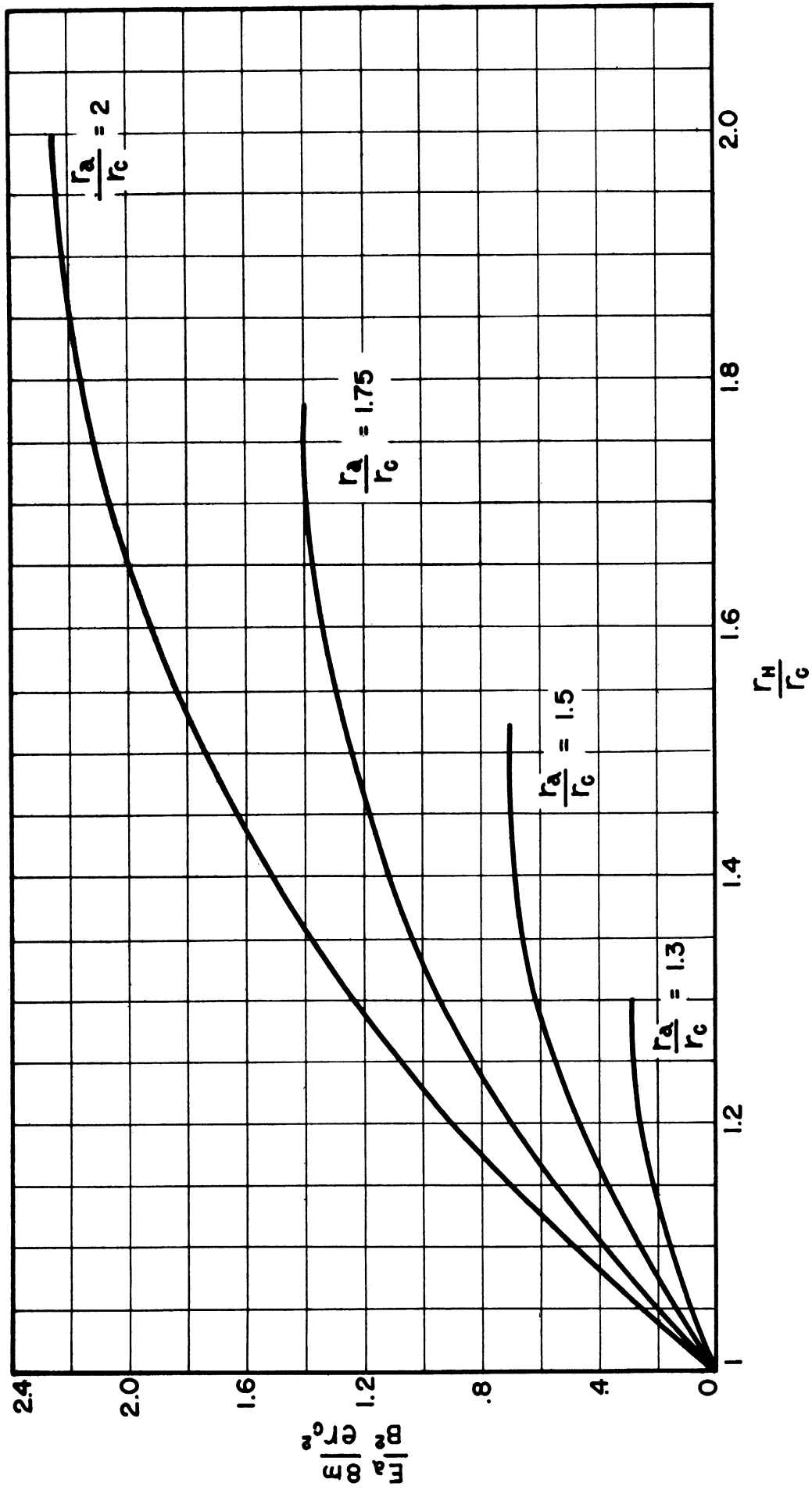


FIG. 13 CASE I. RADIUS OF SPACE CHARGE AS FUNCTION OF E_a/B^2 FOR VARIOUS VALUES OF r_a/r_G FROM EQUATION 5.13.

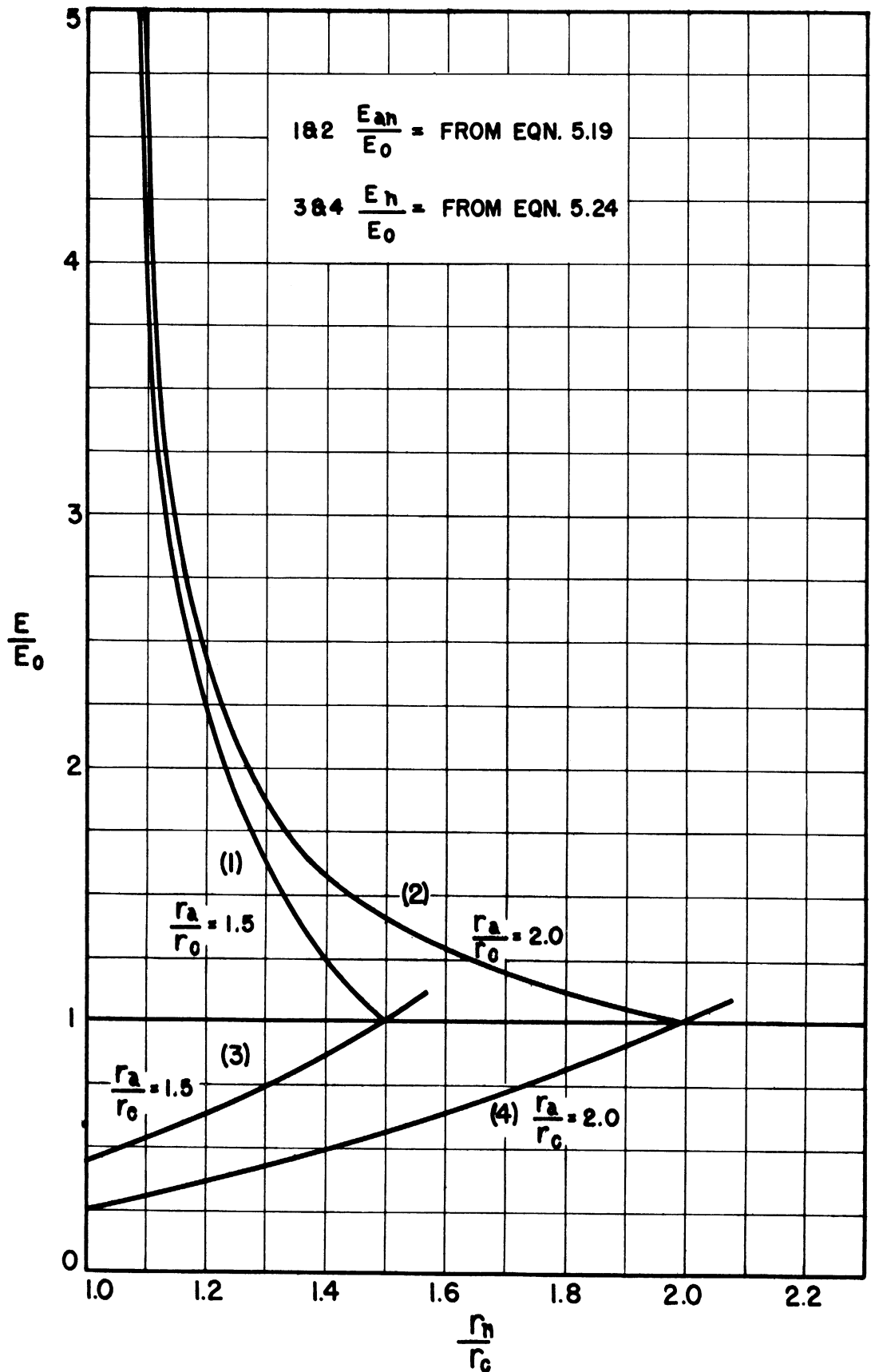


FIG. 14 CASE II ANODE VOLTAGE AND SPACE CHARGE CLOUD BOUNDARY VOLTAGE AS FUNCTION OF RADIUS OF SPACE CHARGE CLOUD BOUNDARY FOR SYNCHRONISM.

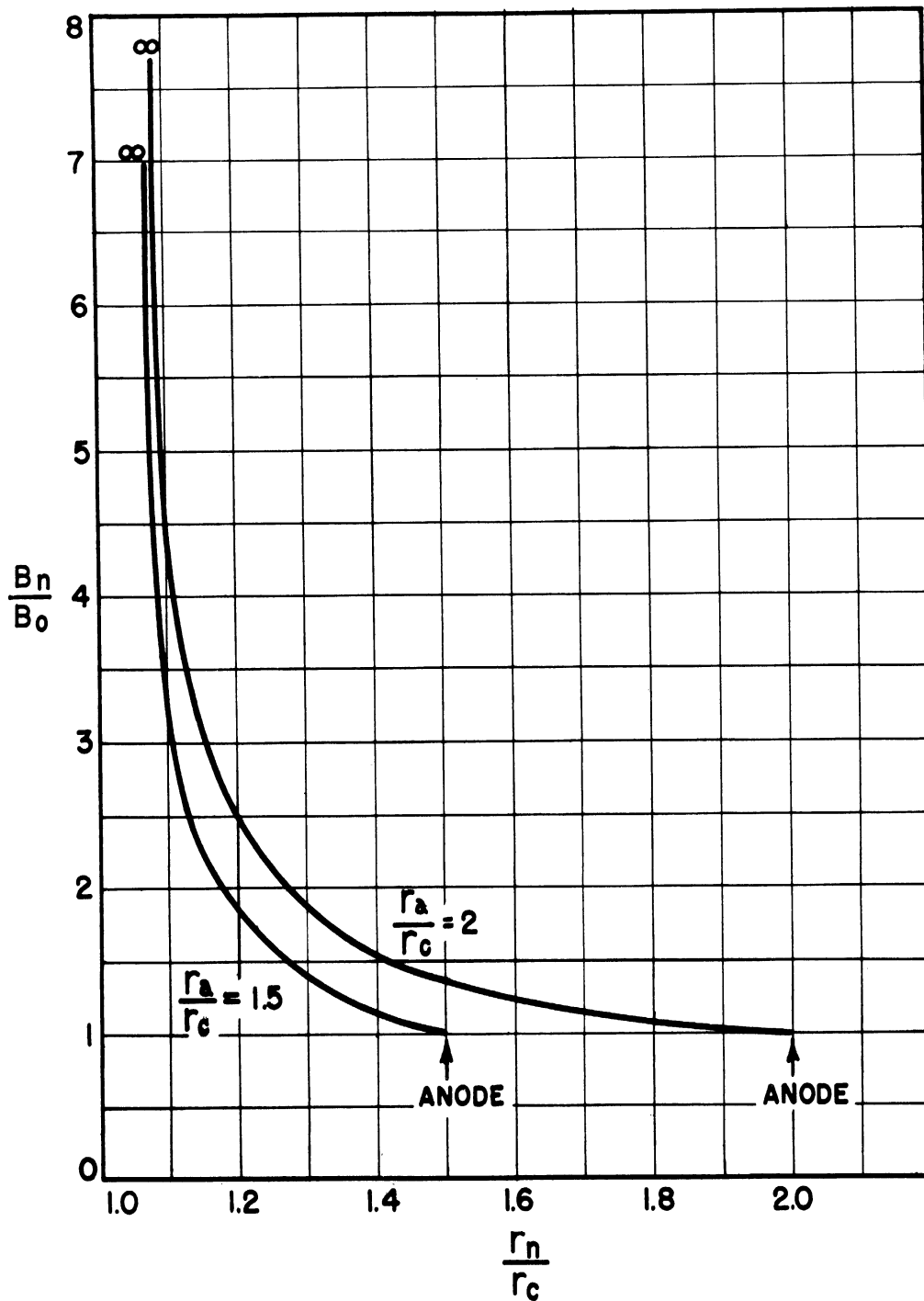


FIG. 15
CASE II MAGNETIC FIELD AS FUNCTION OF RADIUS
OF SPACE CHARGE CLOUD BOUNDARY FOR SYN-
CHRONISM.

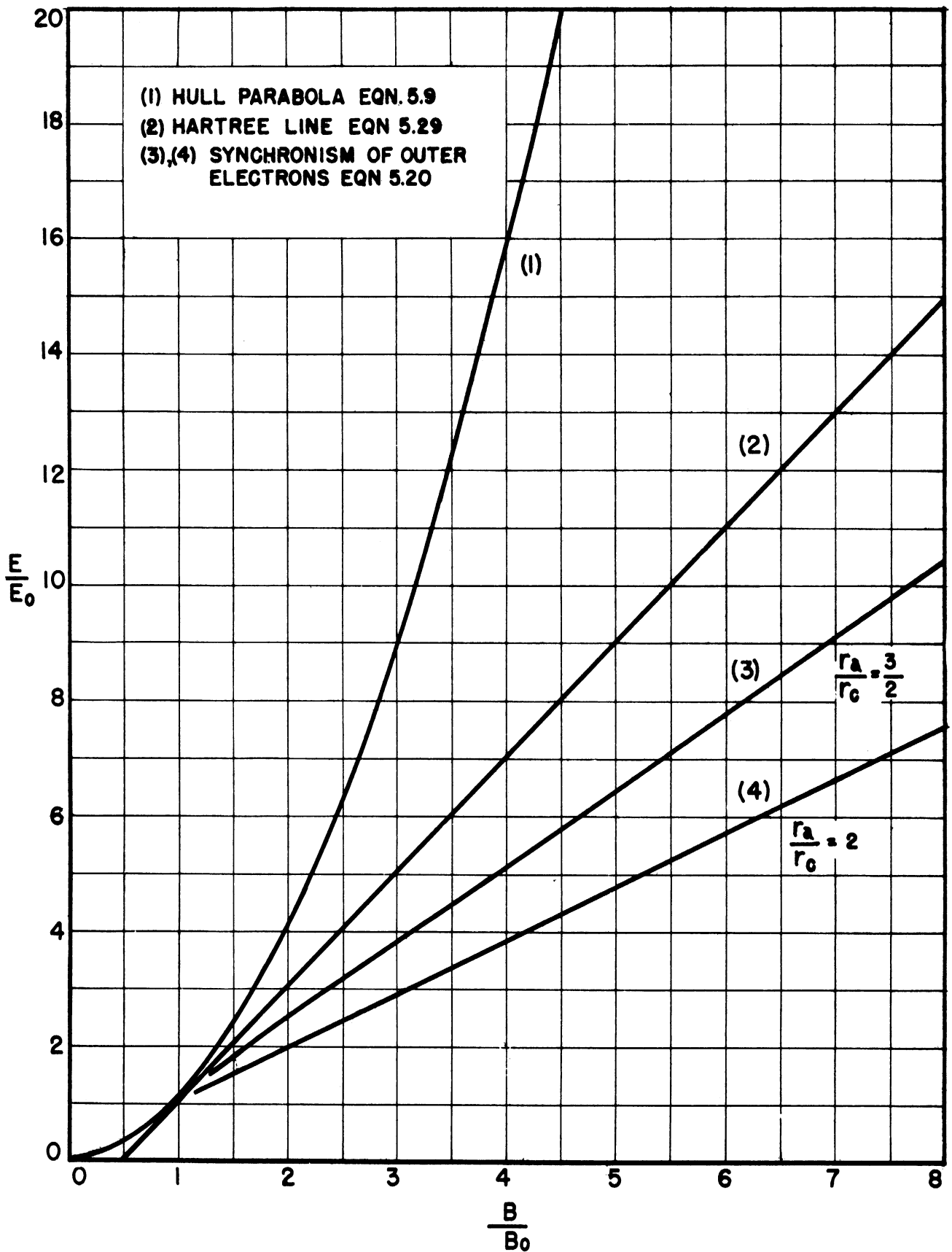


FIG. 16
 CASE II. ANODE VOLTAGES FOR HULL, HARTREE AND
 SYNCHRONOUS BOUNDARIES AS FUNCTION OF MAGNETIC
 FIELD.

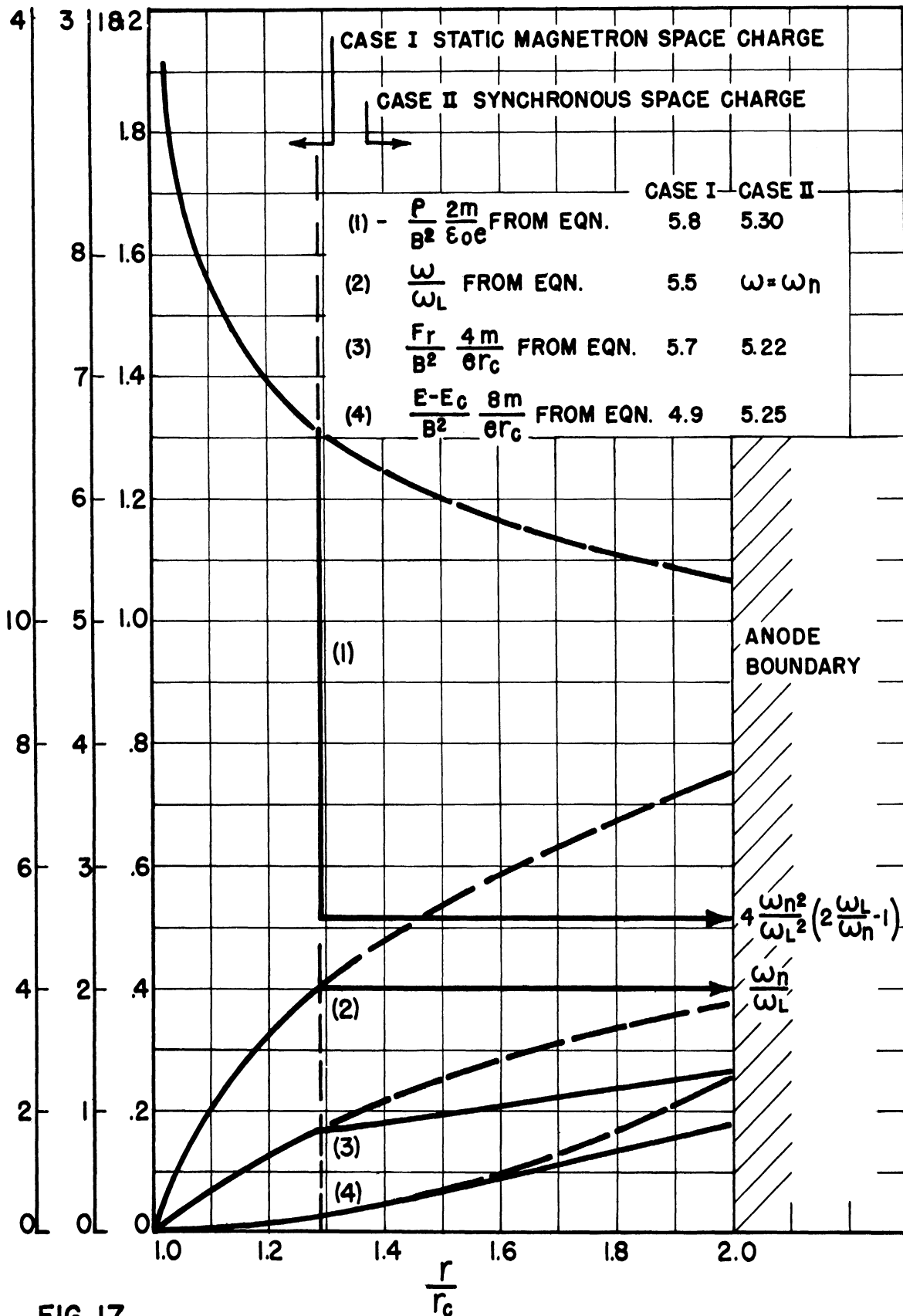


FIG. 17
 CASES I AND II. DISTRIBUTION IN TYPICAL MAGNETRON
 AS HARTREE CLOUD REACHES THE ANODE FOR $\omega_n/\omega_L=4$

NOTE:
 DOTTED CURVES ARE CONTINUATION OF STATIC DISTRIBUTION

The current density is given by the product of the space-charge density and the velocity.

$$\rho \vec{v} = -j \frac{\rho}{\omega_f} \frac{e}{m} \vec{F}$$

From this result one may define a complex conductivity

$$\sigma = - \frac{j\rho e}{\omega_f m}$$

In terms of the complex conductivity the dielectric constant is given by

$$\epsilon_r = 1 - \frac{\sigma}{j\omega_f \epsilon_0} \quad (1)$$

Therefore, in the case of the free electron gas

$$\epsilon_r = 1 + \frac{\rho e}{\omega_f^2 m \epsilon_0} \quad (6.2)$$

Substituting from Equation 5.8 for the space-charge density in a magnetron into 6.2, the following is obtained

$$\epsilon_r = 1 - \frac{B^2 e^2}{2m^2 \omega_f^2} \left[1 + \frac{r_c^4}{r^4} \right] \quad (6.3)$$

This may be written

$$\epsilon_r = 1 - \frac{(\omega_c/\sqrt{2})^2}{\omega_f^2} \left[1 + \frac{r_c^4}{r^4} \right] \quad (6.3a)$$

where ω_c is the cyclotron angular velocity. This value is in agreement with the result obtained by Blewett and Ramo. They assume $r_c^4/r^4 \ll 1$. The dotted curve in Figure 19a is Equation 6.3a plotted with this assumption. For values of $\omega_f < \omega_c/\sqrt{2}$ the space-charge cloud has a negative dielectric constant. When the dielectric constant is negative, the index of refraction is imaginary, and electromagnetic waves cannot be propagated into the cloud and therefore must be reflected from the boundary. The presence of the electron cloud under these conditions should, therefore,

(1) VI-4, p. 203.

have the same effect as the presence of a conductor, or enlarged cathode, in the magnetron. The capacitance between anode and cathode and, therefore, the resonant wavelength of the magnetron is increased. For $\omega_f > \omega_c / \sqrt{2}$, the dielectric constant is positive, but less than one. The effect of the presence of the electrons under these conditions is to reduce the capacitance between anode and cathode, therefore decreasing the wavelength of resonance.

These results, however, must be oversimplified. The fact that a resonance effect is exhibited by electrons in a magnetic field near the cyclotron frequency is well known and used in beam-type modulation devices. We have neglected the effect of the magnetic field in our original Equation 6.1. Blewett and Ramo, in their development using a perturbation method⁽¹⁾, failed to include the effect of the static magnetic field on the perturbation quantities. Specifically, the cross product of the perturbed velocity and the static magnetic field was omitted in the mathematical analysis. The static magnetic field appears only in the relationship for the space charge as in the above development.

It is possible to obtain a first approximation of the effect of the presence of the magnetic field by carrying out a similar derivation to the last with the inclusion of the Lorentz force in the force equation. Figure 18 shows the relative orientation of the field vectors in a magnetron. The magnetic field is perpendicular to the direction of propagation of a wave originating from the anode. The r-f electric field is assumed entirely in the xy-plane and motion of electrons, therefore, entirely in

(1) VI-1.

the xy-plane. This type of problem has been solved in papers on propagation through the ionosphere with the following result⁽¹⁾:

$$\epsilon_r = 1 + \frac{2 \frac{\rho e}{m \epsilon_0 \omega_f^2} \left(\omega_f^2 + \frac{\rho e}{m \epsilon_0} \right)}{2 \left(\omega_f^2 + \frac{\rho e}{m \epsilon_0} - \omega_c^2 (1 \pm 1) \right)} \quad (6.4)$$

If we substitute for ρ as before, letting $1 + \frac{r_c^4}{r^4} = 1$

$$\epsilon_r = 1 - \frac{1}{2} \frac{\frac{\omega_c^2}{\omega_f^2} \left(\omega_f^2 - \frac{\omega_c^2}{2} \right)}{\left(\omega_f^2 - \frac{\omega_c^2}{2} \right) - \frac{\omega_c^2}{2} (1 \pm 1)} \quad (6.5)$$

When the (-) sign is used

$$\epsilon_r = 1 - \frac{1}{2} \frac{\omega_c^2}{\omega_f^2} \quad (6.5a)$$

This is the same result obtained for the case of no magnetic field. With the (+) sign

$$\epsilon_r = 1 - \frac{1}{2} \frac{\omega_c^2}{\omega_f^2} \frac{\left(1 - \frac{1}{2} \frac{\omega_c^2}{\omega_f^2} \right)}{\left(1 - \frac{3}{2} \frac{\omega_c^2}{\omega_f^2} \right)} \quad (6.5b)$$

These results are plotted in Figure 19a. The cause and effects of the \pm sign in similar relationships for ϵ_r are discussed in papers on the ionosphere⁽²⁾. The electromagnetic field is considered made up of two circularly polarized waves of right and left hand polarization. The two polarizations have different orientations with respect to the static magnetic field. This causes one polarization to propagate differently than the other, thus the two values of dielectric constant. The result of most importance to this discussion is that the dielectric constant becomes

(1) VI-6; VI-5, pp. 327-330.

(2) VI-6.

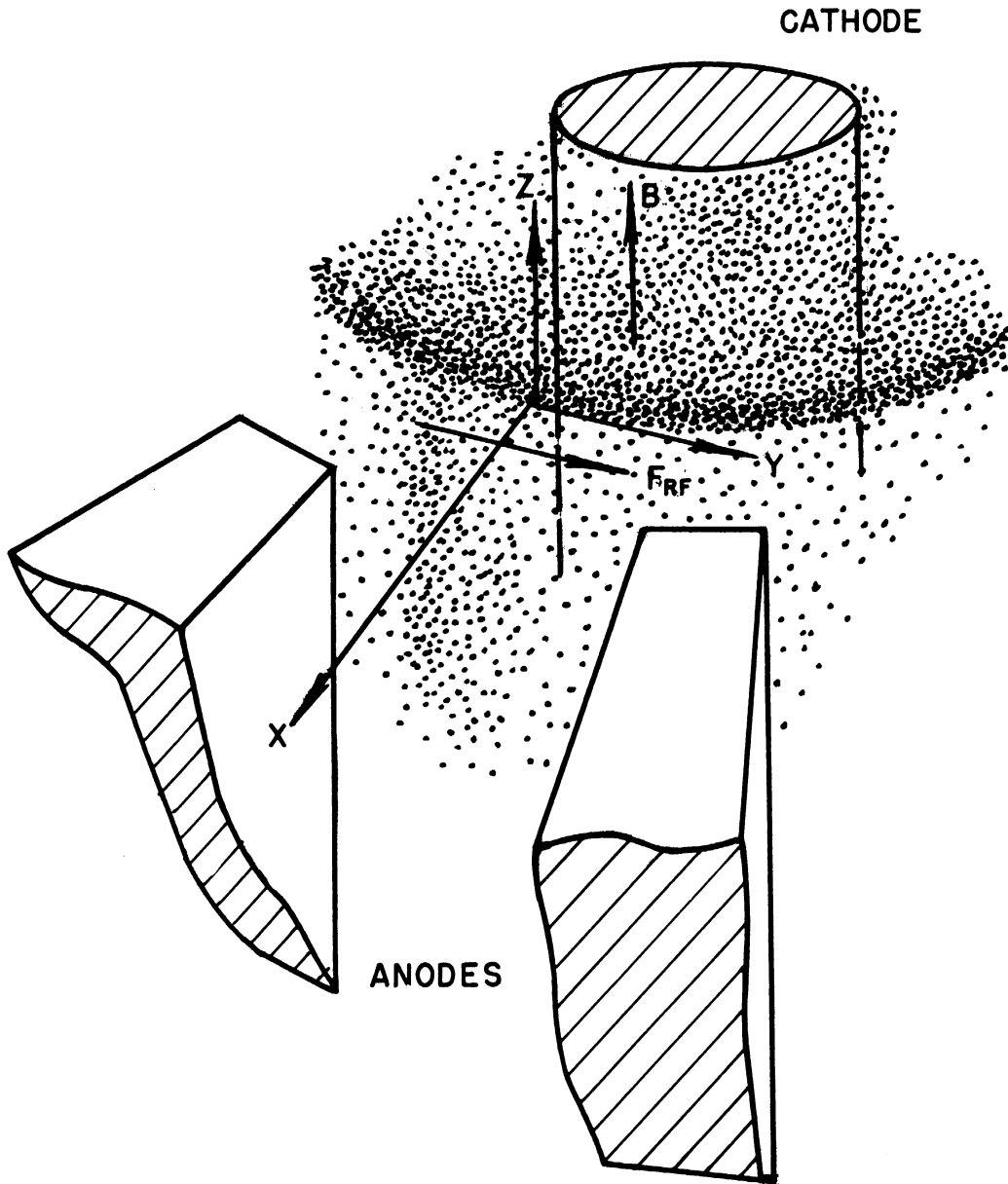


FIG.18 ORIENTATION OF FIELD VECTORS
IN MAGNETRON SPACE CHARGE

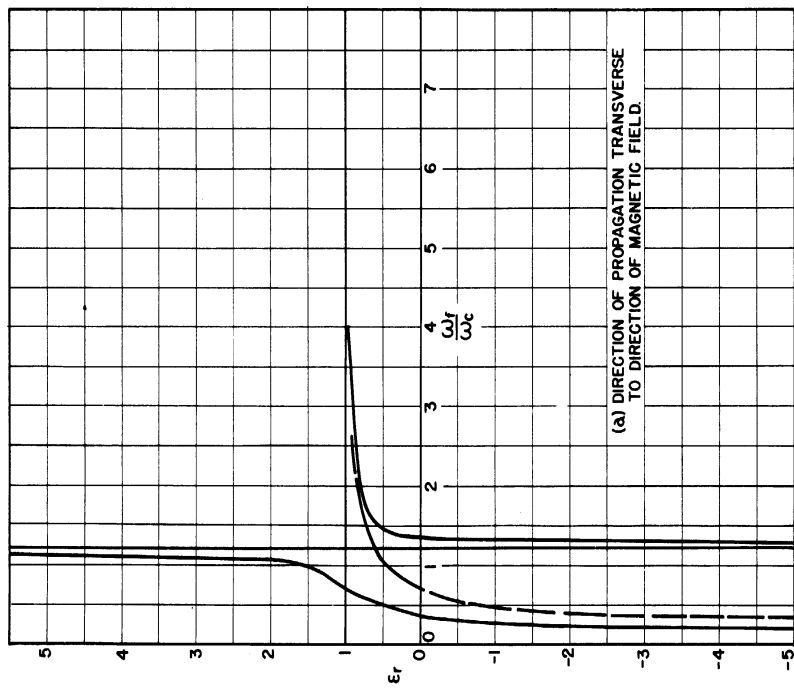
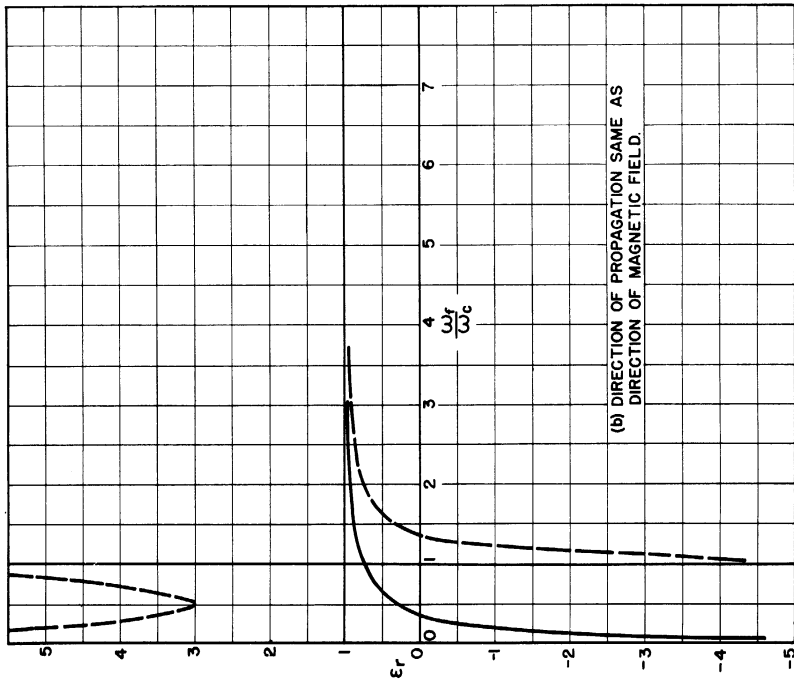


FIG. 19 DIELECTRIC CONSTANT OF MAGNETRON SPACE CHARGE AS FUNCTION OF ω/ω_c

definitely negative at $\omega_f = 0.36 \omega_c$ rather than $\omega_f = 0.707 \omega_c$. This has a bearing on the design of f-m magnetrons which will be discussed in Section 8.

Another case should be mentioned which, although it does not occur in the conventional magnetron, it is of importance in some structures usable for frequency modulation. In this case we assume the direction of wave propagation is the same as the direction of the magnetic field. Under these conditions ϵ_r becomes

$$\epsilon_r = 1 - \frac{1}{2} \frac{1}{\frac{\omega_f}{\omega_c} (\frac{\omega_f}{\omega_c} \pm 1)} \quad (6.6)$$

This result is plotted in Figure 19b. Again we have different dielectric constants for the two circular polarizations of the wave. However, in this case for $\omega_f/\omega_c < .36$ the dielectric constant is positive for one polarization. There is no region in which the dielectric constant is negative for both polarizations. If ω_f/ω_c is made very small, e.g., $\omega_f/\omega_c < .1$, the positive dielectric constant is large enough to cause substantial reflection so that the approximation of the space charge by a conducting surface is probably still valid. No detailed experimental data exist for this case.

The detail of the behavior of the dielectric constant of the space-charge cloud near the cyclotron resonance has not been studied experimentally for either of the cases just discussed. The preceding treatment is probably not correct in this region, because, as the amplitudes of the electron oscillations become larger due to the resonance effect, the damping factor, which was neglected, becomes important. There are also the simplifications of neglecting the fact that the angular velocity of the electrons and of the r-f wave are of the same order of magnitude

and assuming the wave front to be plane. In the more rigorous treatment of Lamb and Phillips⁽¹⁾, the behavior near the cyclotron resonance is described from an impedance point of view for very small sheaths of electrons surrounding the cathode. Their result is the following

$$Z_{el} \cong \frac{F_{\theta}}{H} = \frac{in^2s}{r_c^2 \epsilon_0 \omega_f} \frac{\omega_f^2}{\omega_c^2 - \omega_f^2} \quad (6.7)$$

where s is the thickness of the electron sheath around the cathode. It is assumed that

$$\frac{ns}{r_c} < \frac{\omega_c^2 - \omega_f^2}{\omega_f^2} \quad \text{and } n \neq 0$$

An effective cathode radius may be calculated which when used as a boundary condition obtains the same effect on resonant frequency of the anode block as the condition of Equation 6.7. This is the following

$$r_{c_{eff.}} = r_c \left(1 + \frac{2ns}{r_c} \frac{\omega_f^2}{\omega_c^2 - \omega_f^2} \right)^{\frac{n}{2}} \quad (6.8)$$

This result is in qualitative agreement with the results plotted in Figure 19a. For $\omega_f > 1.36 \omega_c$, cathode diameter is effectively decreased in both cases. (The positive dielectric constant less than one has this effect.) For $\omega_f < 0.36 \omega_c$ the cathode diameter is effectively increased in both cases. For $\omega_f = \omega_c$ the simplified result of the Lamb and Phillips discussion cannot be used.

The restriction on the magnitude of s/r_c is a severe limitation in the practical case of an oscillating magnetron or frequency modulation structure. In either of these cases, s/r_c can approach the magnitude of r_a/r_c . A qualitative physical picture of the behavior of the electrons

(1) VI-3.

near the cyclotron resonance is given in Figure 20. In all cases the angular frequency impressed on the anode is assumed to be the cyclotron frequency. ω is the angular velocity of the outermost electrons. If $\omega \ll \omega_c$ (corresponding to small s) as in Figure 20a, the perturbed electron will execute several cycles in passing a set of anodes. In this case the resonance effect should occur very near the cyclotron frequency. The effect of the steady-state angular velocity is not important. If $\omega = \omega_c/n$ as in Figure 20b, the electron executes a single cycle in just the time it takes it to move, due to the steady-state velocity, from one set of anodes to the next. In the same time, the direction of the field between the next set of anodes has changed to be in phase with the electron oscillation. In the case of Figure 20c, the electron does not execute a single cycle in transit between two anodes and arrives between the next set out of phase with the field. These effects near synchronism ($\omega = \omega_c/n$) possibly can be observed experimentally. To our knowledge extensive data on the cyclotron resonance which might serve to clarify the picture do not exist. At frequencies far from the cyclotron resonance the electrons do not have any natural phase relationship to the r-f field and the amplitude of the oscillation.

7. DISCUSSION OF SPACE-CHARGE BEHAVIOR AND INTERPRETATION OF EXPERIMENTAL EVIDENCE

The analysis presented in the last two sections must not be interpreted in every case as presenting an accurate explanation of behavior in the physically-existent magnetron. On the other hand, it establishes some very useful concepts and important boundaries on actual space-charge behavior. The concepts are useful in explaining the mechanism of the

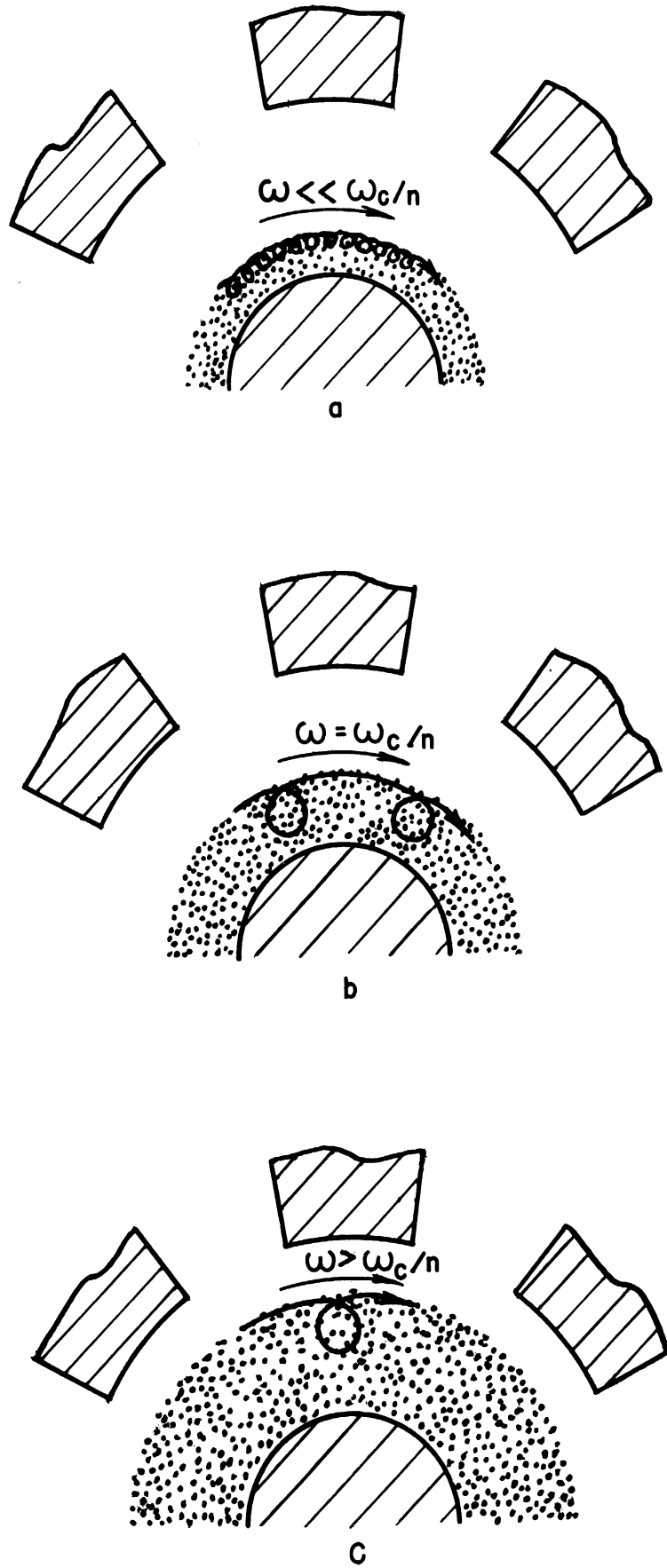


FIG. 20 QUALITATIVE PICTURE OF CYCLOTRON RESONANCE

space-charge behavior. The boundaries are useful in that they place limits on the design of magnetrons.

7a. Hull Voltage: Noise in Magnetrons

We have already pointed out in the last section that the Hull distribution is based on artificial assumptions. It is, however, an important boundary. The Hull Voltage (defined by Equation 5.9 for $r = r_a$) is that voltage above which plate current must be drawn in a magnetron.

We are implying that current might be drawn below the Hull voltage. Experiments indicate in some cases that current starts at voltage as low as one-tenth of the Hull voltage. The fraction seems to depend on the magnetic field used. This should only be possible if electrons were traveling at lower angular velocities than that corresponding to the Hull voltage. If this is the case, the electrons must have given up some of the energy extracted from the d-c field. The electron need only give up an infinitesimal fraction of its energy in the first trip out from the cathode to lose enough momentum to prevent its return to the cathode. If it does not return in its first trip, it will keep circulating indefinitely. In this continuing process, it is almost inconceivable that the eventual loss of energy would not result in some electrons being found outside the radius defined by the Hull condition.

The ways in which electrons could lose energy to the surroundings are the following:

- (a) Radiation losses - insignificant
- (b) Collisions with large ions in the interaction space
- (c) Loss of energy to noise voltages generated in the tube

Either (b) or (c) or both could account for the relatively large currents

which sometimes exist in the region below the Hull voltage or before oscillation starts. In either case these currents should be accompanied by the development of high noise levels in the magnetron. Some measurements have been made which indicate a positive effect of presence of large ions on noise level⁽¹⁾. Other measurements show that the noise output in a preoscillating magnetron increases exponentially with plate current until the magnetron shows a definite tendency to start oscillation⁽²⁾. If the magnetron space charge can supply amplification of noise, and theoretical and experimental evidence indicate that it might, the gap between theoretically produced noise level in the region of the cathode and the observed noise output is filled.

A more detailed study of the causes of plate current existing below the Hull voltage in a non-resonant structure might give a satisfactory explanation of the apparently inherent noisy character of the magnetron. This is of course very important when they are to be used for communication purposes.

7b. Hartree Voltage: Oscillation

The definition of the Hartree voltage by Equation 5.29 has a similarity to the definition of the Hull voltage. It is also based on artificial assumptions, but it is also a very important boundary. It is assumed that kinetic energy of the electrons throughout the space-charge cloud is entirely of angular velocity. Therefore, the electrons arrive at the anode with the minimum possible energy. R-f voltage need not

(1) X-1.

(2) X-2.

exist for the stable existence of the Hartree distribution. If oscillation is to be supported even with an infinitesimally small plate current, the Hartree voltage must be exceeded. The Hartree voltage is therefore that voltage below which oscillation cannot take place in an ideal magnetron. Departures from this boundary in the direction of lower voltages should be due to non-ideal qualities of the magnetron. For instance, in a multivane magnetron the d-c field cannot be considered entirely radial; magnetic field is usually not quite uniform, cathode structures and straps cause end distortion of the electric field in the interaction space. Magnetrons usually start oscillation very slightly below the Hartree voltage. Above the Hartree voltage the question as to whether the magnetron will oscillate or will not oscillate has to do with the circuit parameters, shunt impedance, loaded Q, etc. These factors are not taken into consideration in the development of the Hartree relationship. The connection between the Hartree equation and the circuit is through ω_n . The maximum angular velocity of the electrons within the interaction space is considerably larger than ω_n before oscillation starts. As the voltage reaches the Hartree boundary it becomes possible for oscillation to be supported. In the transient condition as oscillation begins, all of the electrons which had been traveling at velocities greater than ω_n give up their energy and reach the anode. As oscillation becomes steady the exchange of energy is continuous. The electrons continually extract energy from the d-c field and transfer it to the r-f field. The r-f field is alternately opposing and aiding the motion of the electrons so, if we place ourselves in a moving frame of reference, moving with the traveling wave, we would see the spokes begin to form on the space-charge cloud where the electrons are being slowed to synchronism. In the oscillating

magnetron these spokes must always reach out to the anodes since oscillations cannot be supported unless plate current is drawn. In the magnetron undergoing a hot impedance test the spokes can form due to the presence of an impressed r-f field.

7c. Frequency Pushing

Frequency pushing is explained qualitatively on the basis of these ideas. The Hartree voltage is nearly proportional to ω_n . This can be seen by rewriting the Equation 5.29 in terms of ω_n . The second term in this equation is usually less than a tenth of the first.

$$E_a = \frac{r_a^2}{2} \omega_n B \left[1 - \frac{r_c^2}{r_a^2} \right] - \frac{1}{2} \frac{m}{e} \omega_n^2 r_a^2 \quad (5.29a)$$

The lowest value of ω_n which satisfies this equation and for which the space-charge cloud can compensate for the losses and phase angle in the resonant circuit will give the value of E_a for which the magnetron can start oscillating. The generated frequency will be lower than the cold resonance frequency of the tank circuit by a margin of the order of $1/Q$. The impedance offered by the tank circuit is almost a pure inductance and power delivered from the electron swarm is small. As the anode voltage is increased, more electrons will be traveling fast enough to give energy to the r-f field. This results in more power output and an increase in frequency. The phase angle between the r-f voltage induced in the tank circuit and the current from the equivalent current generator in Figure 2b is decreased. Figure 4 shows experimental data on frequency pushing.

In Figure 6 these data are compared with hot impedance test results. It should be noted that the whole pushing curve is shifted from

the cold resonant wavelength of the magnetron by an amount which compares with the shift in the hot impedance test results. This means that the resonant wavelength of the active magnetron is shifted to longer wavelengths by the passive effects of the space-charge cloud expanding within the magnetron. These effects are explained in Section 7e. When the magnetron starts oscillating the active effects described above cause the resonant wavelength to shift in the opposite direction. The lowest value reached is still considerably greater than the cold resonant wavelength due to the effect of the space charge.

The decelerating effect of the increasing r-f voltage tends to counteract the increase in angular velocity and may be an explanation for the fact that pushing curves tend to double back in frequency at higher voltages.

7d. Space-Charge Effects on Rieke Diagram

The cause of frequency pushing is, therefore, the tendency for the electron swarm to increase in velocity as anode voltage is raised; i.e., the frequency of the current generator is a function of the power output of the generator. The power output is determined by the load on the generator. We have mentioned in Section 3 that experimental evidence of Rieke diagrams indicates the electronic susceptance to be a function of the load conductance on the magnetron. Variation of the conductive portion of the magnetron load without change in the susceptive portion varies the form of the resonance curve without changing its position on the frequency axis. The rotating swarm of electrons must adjust itself to meet the conditions of negative conductance and phase relationship to the r-f voltage imposed by the resonant circuit. In addition, the

changing r-f voltage caused by variation in load will react on the electron swarm. This combination of causes must have a very complex, but not very large, effect upon the frequency of oscillation. Further complication results from the fact that a particular value of load conductance (a particular form of the resonance curve) allows maximum efficiency of energy transference from the electron swarm to the r-f field. This is the condition of optimum shunt impedance. The characteristics of the optimum condition are understood for conventional oscillators employing triode or tetrode vacuum tubes but still not satisfactorily explained in the case of the magnetron oscillator.

7e. Hot Impedance Measurements

Behavior in the non-oscillating magnetron is discussed on a slightly different basis than is used for the oscillating magnetron. The spontaneity of the formation of the spokes is not present. The automatic adjustment of the phase angle to suit the needs of the resonant circuit is not necessary. This was suggested in Section 4. The effect of the electrons on the resonant circuit can therefore be looked upon as a passive rather than an active effect. This is not entirely true as is immediately seen upon examination of Figures 6 to 10. The increase in Q , for example, must be an active effect.

In Figure 7 the variation of λ_0 , Q_0 and G_0 is plotted against plate voltage for two values of r-f voltage impressed upon the anode structure. The general form of the curves is seen to be the same with a reduction in Q as the voltage is raised. The Q_0 curves are relatively flat up to about 700 volts. This indicates that there is no change in the conductive characteristics of the space charge in this region. Above

700 volts, the Q_0 begins to rise sharply. At the point of oscillation it would, ideally, go to infinity as the conductance goes to zero. This point occurs at about 900 volts. This behavior means that in the region between 700 and 900 volts space charge is contributing energy to the r-f field and therefore the spokes must form on the outside of the Hull space-charge cloud. When the Q_0 curve intersects with the cold Q_0 line the space charge is contributing just enough negative conductance to compensate for losses within the circuit due to bombardment of the cathode and collisions with large ions which may be present. The further increase in Q_0 represents compensation for copper losses in the resonant circuit. The reduction of the Q_0 in the flat portion of the curve is due to increase in losses due to back bombardment as r-f voltage is raised. The data in Figure 8 show how the Q_0 varies with r-f voltage for a value of anode voltage in the flat portion of the curve. The losses are going up rather rapidly with the increasing r-f voltage. This effect is probably due to an increase in the energy spent in back bombardment of the cathode. These losses may impose a serious limitation on the use of this effect in frequency modulation devices. The variation in λ_0 with r-f voltage is not particularly significant.

Quantitative discussion of the variation of λ_0 with plate voltage is possible in terms of the results of Sections 5 and 6. For this purpose, we will use the data presented in Figure 9. The characteristics of the magnetron used in this experiment are summarized in Table 1. The purpose of these two sets of measurements was to obtain data for the two cases discussed in Section 5. In Figure 9a, the magnetic field of the magnetron is less than B_0 . Thus the outer electrons in the swarm do not reach synchronism with the resonant frequency of the circuit before they

reach the anode. The magnetron cannot oscillate. The space charge should behave as in a magnetron diode and obey the conditions of Case I. In Figure 9b, the magnetic field is greater than B_0 . The electrons can reach synchronism and the magnetron can oscillate. When hot impedance tests are made, as soon as the radius of synchronism r_n is exceeded, the electrons can begin giving energy to the r-f field. In this way they may be slowed to synchronism and the spokes, or a second cloud, can form outside r_n which expands more rapidly with voltage than the inner cloud. This cloud forms according to the conditions of Case II. When the outer boundary of this cloud reaches the anode, the magnetron can start oscillating. Before it reaches the anode it might have an effect on resonant frequency of the anode block.

In order to calculate the effect which the space-charge cloud has on the resonant frequency of the circuit, we use the results of Section 6. At the magnetic field used in taking data for the curves in Figure 9a, the value of ω_p/ω_c is approximately 3. The dielectric constant of the space charge is, from Figure 19, positive and slightly less than unity. The effect of the electrons, if any, should be to reduce the capacity between anode and cathode and therefore decrease the resonant wavelength. Such an effect is observed in Figure 9a. The wavelength decreases until plate current is drawn. After plate current is drawn the whole volume between anode and cathode is filled with space charge and any further change in resonant wavelength must come from actual change in the dielectric constant of the space charge. Before plate current is drawn, the expansion of the cloud has the predominant effect. If we assume that lumped-constant circuit theory can be used, the approximate change in λ_0 may be calculated. This is a good assumption in the case

Table 1. Data on Model 3 Interdigital Magnetron
 Constructed at the University of Michigan

Anode radius	r_a	.45 cm.
Cathode radius	r_c	.27 cm.
$\frac{\text{Anode radius}}{\text{Cathode radius}}$	$\frac{r_a}{r_c}$	1.66
Number of anode fingers	N	12
Length of cathode	L	.66 cm.
Length of anode finger	l	.834 cm.
Spacing between anode fingers	d	.018 cm.
Outer radius of anode	R_a	.900 cm.
Inside radius of outer cavity wall	R_c	1.90 cm.
Height of cavity	h	.95 cm.
Capacitance between anode sets	C_a	5.5×10^{-12}
$\frac{\text{Capacitance to cathode}}{\text{Total anode capacitance}}$	α	.045
Voltage for synchronism at anode	E_o	200 volts at 17 cm.
Magnetic field for synchronism at anode	B_o	330 gauss at 17 cm.

of the interdigital magnetron used in these experiments.

The total capacitance in the resonant circuit includes the capacitance between anode and cathode. The latter is the portion which is varied by the presence of the electrons. Let α represent the percentage correction which must be applied to the ordinary circuit capacitance C to account for the capacitance between anode and cathode. The resonance wavelength in the absence of the electrons is given by

$$\lambda_0 = 2\pi c \sqrt{LC (1 + \alpha)} \quad (7.1)$$

In the presence of electrons completely filling the space the resonance wavelength becomes

$$\lambda_0 + \Delta\lambda_0 = 2\pi c \sqrt{LC (1 + \alpha \epsilon_r)} \quad (7.2)$$

Here ϵ_r is the dielectric constant to be taken from Figure 19a. In this case, we are only interested in positive values less than one. Otherwise, the approximations made in the following discussion will not be correct. α is of the order of five per cent or less.

Dividing Equation 7.1 by Equation 7.2, we have

$$\begin{aligned} 1 + \frac{\Delta\lambda_0}{\lambda_0} &= \sqrt{\frac{1 + \alpha \epsilon_r}{1 + \alpha}} \\ &= \sqrt{1 + \frac{\alpha(\epsilon_r - 1)}{1 + \alpha}} \end{aligned}$$

Assuming $\alpha \ll 1$ this becomes

$$\boxed{\frac{\Delta\lambda_0}{\lambda_0} = \frac{\alpha}{2} (\epsilon_r - 1)} \quad (7.3)$$

For the magnetron used in these experiments,

$$\alpha = 0.045$$

and under conditions of the experiment, $\omega_f/\omega_c \cong 3$. In this region,

$$(\epsilon_r - 1) \approx -\frac{1}{2} \left(\frac{\omega_c}{\omega_f}\right)^2$$

Therefore,

$$\epsilon_r - 1 = -0.055$$

The change in λ_0 to be expected is therefore

$$\Delta\lambda_{0\text{calc.}} = -0.021 \text{ cm.}$$

The observed change between 0 and 75 volts (the Hull voltage) is

$$\Delta\lambda_{0\text{obs.}} = -0.025 \text{ cm.}$$

taken from the smooth curve. The Hull voltage is selected because at this point the space should just be filled with the approximate space-charge density used in derivation of the formula for ϵ_r .

At the magnetic field used in taking data for the curves in Figure 9b, the ratio of $\omega_f/\omega_c = 0.37$. This is on the border of the point where the dielectric constant of the space charge in the Hull cloud becomes negative. The dielectric constants for the two wave polarizations are definitely of different magnitudes. If we assume the wave is totally reflected, the Hull cloud will behave effectively as a conducting surface. The effect of the space charge in the outer or Hartree cloud may be neglected. The space-charge density in this region is less than the space charge in the inner cloud by a factor given in Equation 5.31. In this magnetron $n = 6$; therefore, the ratio is the following

$$\frac{\rho_{\text{Hull}}}{\rho_{\text{Hartree}}} = 10$$

The space-charge cloud in spite of its relatively small density might be expected to have an effect due to its synchronous characteristics near the voltage at which oscillation starts.

The radius of the space charge in the inner cloud is given by reference to Figure 13. In this case,

$$E_a = 1490 \text{ volts}$$

$$B = 1700 \text{ gauss}$$

$$r_c = 0.27 \text{ cm.}$$

$$\frac{r_a}{r_c} = 1.66$$

Therefore,

$$\frac{E_a}{B^2} \cdot \frac{8m}{erc^2} = 0.32$$

and from Figure 13

$$\frac{r_H}{r_c} = 1.11$$

The capacitance between anode and cathode will be a function of the following form:

$$C_c = \frac{K}{\ln r_a/r_c} \quad (7.4)$$

where K is a function of r_a/r_c because of fringing effects around the anodes. The percentage change in effective capacitance to the cathode is therefore the following if we consider r_H as a reflecting surface.

$$\frac{\Delta C_c}{C_c} = \frac{\frac{K_H}{\ln r_a/r_H} - \frac{K_c}{\ln r_a/r_c}}{\frac{K_c}{\ln r_a/r_c}}$$

$$\boxed{\frac{\Delta C_c}{C_c} = \frac{K_H \log r_a/r_c}{K_c \log r_a/r_H} - 1} \quad (7.5)$$

and for values of $\Delta C_c/C$ of the order of $1/20$ α or less

$$\frac{\Delta \lambda_o}{\lambda_o} \cong \frac{1}{2} \alpha \times \frac{\Delta C_c}{C_c}$$

where α has the same meaning as in the previous discussion. We consider $K_H = K_c$ constant in the present case. This should be a safe assumption for a 10 per cent change in effective cathode radius. The resultant value of $\Delta\lambda_0$ is therefore

$$\begin{aligned}\Delta\lambda_{0\text{calc.}} &= \frac{1}{2} \times 0.045 \times 0.25 \times 16.9 \text{ cm.} \\ &= 0.095 \text{ cm.}\end{aligned}$$

This value is in very close agreement with the total observed change, considering that the error in measurement of λ_0 is of the order of 0.01 cm.

$$\Delta\lambda_{0\text{obs.}} = 0.11 \text{ cm.}$$

Judging from this calculation and general form of the experimental curve, we would conclude that the reactive effects of bunching before oscillation are very small, if any, and that the entire wavelength shift before oscillation is due to the expansion of the inner space-charge cloud. When oscillation begins, the pushing effect becomes predominant as was described in Section 7c in the interpretation of Figure 6.

In order to complete the discussion something should be said about the behavior at the cyclotron resonance shown in Figure 10. We do not feel, however, that sufficient data exist, nor that the theory is sufficiently well formulated to do more than point out that the form of the curve in Figure 10 is in qualitative agreement with the predictions of the theory and that the magnetic field for which resonance occurs agrees closely with the theoretically predicted value

$$\begin{aligned}B_c &= \frac{2\pi c}{\lambda_c} \frac{m}{e} \\ &= 630 \text{ gauss}\end{aligned}$$

for $\lambda_c = 16.9$ cm. The shift of the whole resonance from the λ_0 for zero

plate voltage is probably due to the expanded cloud.

As has been stated before, the use of the cyclotron resonance is undesirable and should be unnecessary in the frequency modulation of magnetrons by a space-charge cloud.

8. GENERAL DISCUSSION OF FREQUENCY MODULATION METHODS; DESIGN CRITERIA FOR MULTIANODE STRUCTURES

Of the four general methods of electronic frequency modulation mentioned in Section 1, two can immediately be discarded as impractical in the magnetron. These are: modulation obtained through effects due to the same electrons which are the source of oscillation, and modulation caused by frequency pulling. Both of these types of modulation are accompanied by amplitude modulation, in the first case due to the reverse of the frequency pushing effect, and in the second case due to the interrelation of space-charge conductance and susceptance exhibited in the Rieke diagram.

Of the remaining two possibilities, the use of a second source of electrons within the resonant circuit, producing a controllable reactive effect, is definitely superior in theory to the "reactance tube" method in which a reactive effect due to electrons is introduced into a structure external to the magnetron resonant circuit. This has been discussed in considerable detail in a report of R.C.A. Laboratories⁽¹⁾. They draw the general conclusion that a given electronic susceptance can produce a larger frequency deviation if used inside the magnetron resonant circuit. Known exceptions to this statement have undesirable properties of limited range of modulation, power absorption or instability.

(1) VIII-1.

In practice, however, there are obvious difficulties in physical realization of a device containing a source of electrons which causes oscillation and a second source of electrons which produces modulation. Therefore, if it is possible to obtain a sufficiently large electronic susceptance, use of the "reactance tube" method should not be disregarded. In the present state of the art, the limitation is still the amount of electronic susceptance available. We have therefore limited our thought to devices in which the electrons produce a reactive effect within the resonant circuit of the magnetron. The methods of producing the electronic susceptance are of course applicable to either type of device if tube geometries and circuitry can be constructed which will make use of the susceptance.

The use of an electronic susceptance and a separately controlled electronic generator of oscillation in the same magnetron resonant circuit implies the existence of either separate cathodes or separate sets of anodes or both. The structures utilizing spiral-beam modulation are an example of the first. In this case, a beam of electrons from an auxiliary cathode is injected between vane tips in a vane-type magnetron. The magnetic field is adjusted to the cyclotron resonance so that the small space-charge densities in the beam by relatively large amplitude of oscillation can cause an appreciable effect on frequency. Frequency deviations of the order of 1 per cent have been obtained in this way on relatively low frequency magnetrons (1000 mc)⁽¹⁾. For this deviation, several beams must be used.

(1) VIII-4.

There is no particular advantage to the second type of structure. In order to obtain modulation in a device with two anodes and a single cathode, either one anode is insulated from the other to allow application of a modulation voltage isolated from the d-c voltage, or some sort of grid structure must be incorporated within the second anode. At frequencies above 2000 mc the complexity of such structures increases rapidly. By-pass paths for the r-f must be provided within the vacuum envelope and, if a magnetic field is used in the modulation device, the use of a grid becomes limited.

The third method of supplying modulation is the most flexible. The two anodes may be tied together for r-f and modulation applied to the second cathode or set of cathodes. The anode structure and interaction space in the modulator are designed differently than in the oscillator so that parasitic oscillations in the modulator structure are reduced to a minimum.

The theory developed in Sections 5 and 6 and the experimental results analyzed in Section 7e suggest that a magnetron-type space charge can be used to furnish electronic control of frequency. Frequency shifts of the order of 8 per cent at 500 mc have been obtained using split-anode magnetrons⁽¹⁾. The space charge may be used within a multianode structure attached to the resonant circuit of the magnetron. The theory which has been developed can be used as a basis for convenient design criteria by which anode structure and interaction space designs can be determined which obtain maximum benefit of the space charge and do not permit oscillation.

(1) I-2.

In the first place, if we wish to make use of the properties of a space charge of negative dielectric constant we have the condition

$$\omega_f < 0.36 \omega_c \quad (8.1)$$

This is obtained from Figure 19a. If we wish to place the further restriction that the magnetron does not oscillate, we have the condition

$$B < B_0 \quad (8.2)$$

If 8.1 and 8.2 are combined so that the structure will not oscillate and the space charge will cause total reflection, we obtain the following

$$\omega_f < 0.36 \omega_c = 0.36 \frac{Be}{m} < 0.36 \times B_0 = 0.36 \times \frac{2\omega_f}{n} \frac{1}{1 - \frac{r_c^2}{r_a^2}}$$

which results in the simple criterion

$$1 - \frac{r_c^2}{r_a^2} < \frac{0.72}{n} \quad (8.3)$$

or

$$\frac{r_a}{r_c} < \sqrt{\frac{1}{1 - \frac{0.72}{n}}} \quad (8.3a)$$

This last equation gives the following values of r_a/r_c for various values of n .

$n =$	$r_a/r_c <$
1	1.88
2	1.25
3	1.15
4	1.1
5	1.08
6	1.06

Spacing requirements impose a limitation on the value of r_a/r_c which can be used and therefore on n . For example, if the cathode diameter is of

the order of 1/2 to 1 centimeter, $r_a/r_c < 1.15$ begins to be impractical. Therefore, $N = 2n = 6$ is the largest practical number of anodes. To be on the safe side, $N = 4$ or even $N = 2$ should be used if possible.

If it is desired to make use of the space charge with a positive dielectric constant less than unity the following criterion may be used.

$$\omega_f > 1.36 \omega_c \quad (8.4)$$

ω_f should not be too much in excess of ω_c ; otherwise ϵ differs so little from unity that the change in susceptance due to the space charge will not be appreciable. At most the presence of space charge of these characteristics can do no more than cancel the effect of the cathode. The value of ω_f/ω_c might arbitrarily be limited to less than 2 for this case. If this is done, we have as before

$$1 - \frac{r_c^2}{r_a^2} < \frac{4}{n} \quad (8.5)$$

or

$$\frac{r_a}{r_c} < \sqrt{\frac{1}{1 - \frac{4}{n}}} \quad (8.5a)$$

This imposes no serious restriction on r_a/r_c and is actually satisfied in most conventional c-w magnetrons operating at wavelengths greater than six centimeters.

The relative merits of these two types of behavior under conditions of high r-f voltage are not yet experimentally determined. On paper the use of space charge of negative dielectric constant can produce an infinite change in λ_0 whereas the space charge of positive dielectric constant can only cancel the effect of the cathode. This latter, of course, can be two to five per cent. The linearity of frequency change

and losses under the influence of high r-f voltage might give preference to the latter method. This remains to be seen.

The final problem of design is to incorporate such a space charge within a device which is reasonably easy to assemble, contains adequate provision for power dissipation, and is free from unwanted modes of oscillation. It is also desirable in most cases that the device be tunable and stable in frequency and that modulation be linear with negligible amplitude modulation. In the next section, some particular structures which look promising are suggested.

9. SUGGESTED GEOMETRIES FOR F-M MAGNETRONS

Even when the type of space-charge reactance and the general method of introducing the reactance is selected there remain a multitude of possibly fruitful approaches to the problem of frequency modulation of the magnetron. These depend on the frequency range, power output, tunability, cooling methods and other electrical specifications and structural requirements.

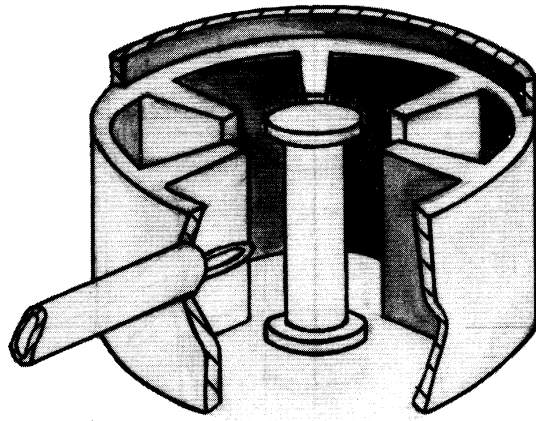
The geometries suggested in the following paragraphs have been built around the use of the interdigital magnetron. This type of magnetron has been in the course of development and experimental use for five or six years. At the close of the war promising results were just being obtained with c-w tubes having power outputs of the order of 50 watts. Efficiencies however were low. The reasons for the low efficiencies which are given below were discovered shortly after the close of the war, making possible the construction of high-power high-efficiency interdigital

magnetron⁽¹⁾. Recently a tunable interdigital magnetron, designed and constructed in this laboratory, has been operated at 16 cm. with 500 watts c-w output at efficiencies over 70 per cent. This magnetron is operated in the lowest order mode rather than the higher order modes previously used. The difficulty with this mode has been a very strong coupling to the cathode circuit inherent in the conventional interdigital magnetron. Coupling of power out the cathode leads diverts power from the true output circuit and, in some cases, may load the tube so heavily in the lowest order mode that it will not operate in this mode at all. In higher order modes the coupling to the cathode line is not present. In the magnetron mentioned above power was prevented from being lost out the cathode lead by chokes appropriately placed within the tube.

Figure 21 shows schematically the interdigital magnetron structure in comparison with the vane-type magnetron. When the lowest order mode is used the teeth on the interdigital anode act as capacitances in the resonant circuit of the magnetron. The cavity surrounding the teeth provides the inductance. If this cavity is considered as a section of radial transmission line loaded at the center by the capacitance of the teeth and short circuited at the outer boundary of the cavity, the cavity radius for a given resonant wavelength and loading capacitance may be calculated as follows⁽²⁾. The input impedance of the radial transmission line formed by the cavity calculated at the outer radius of the anode teeth is given by

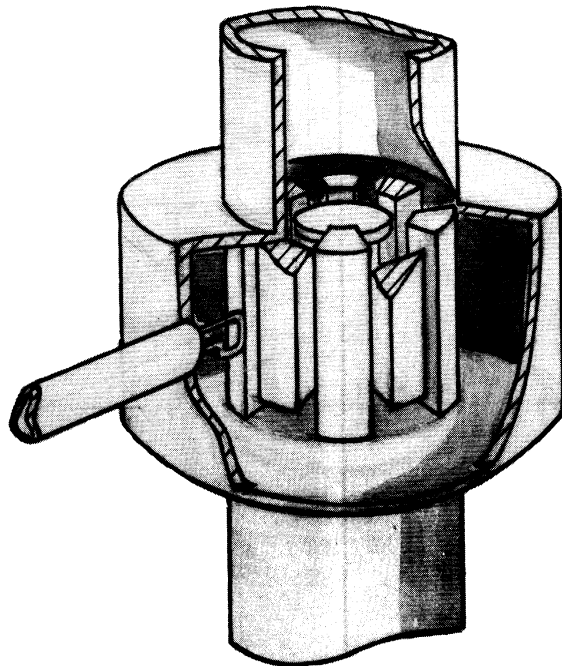
(1) IX-3; IX-4.

(2) IX-5, pp. 406-408, 358.



a

VANE TYPE MAGNETRON



b

INTERDIGITAL MAGNETRON

FIG. 21 COMPARISON OF INTERDIGITAL MAGNETRON
STRUCTURE WITH VANE TYPE STRUCTURE

$$Z_{in} = -j \frac{hZ_{oa} \sin(\theta_a - \theta_c)}{2\pi R_a \cos(\psi_a - \theta_c)} \quad (9.1)$$

Z_o , θ and ψ are functions of $2\pi r/\lambda$ given in Figure 22. Z_{oa} is the input impedance of the radial transmission line at R_a . θ_a and ψ_a are quantities defined at R_a . θ_c is defined at R_c . h , R_a and R_c are the height of the cavity, inner radius of the cavity (or outer radius of the tooth structure) and outer radius of the cavity respectively.

At resonance the impedance defined by Equation 9.1 must be equal to $\lambda_o/2\pi cC_a$ where C_a is the capacitance of the tooth structure. If this equality is solved for θ_c and therefore R_c the following results

$$\theta_c = \tan^{-1} \frac{\sin \theta_a + \frac{\lambda_o R_a}{c C_a Z_{oa}} \cos \psi_a}{\cos \theta_a - \frac{\lambda_o R_a}{c C_a Z_{oa} h} \sin \psi_a} \quad (9.2)$$

The smallest value of θ_c must be used. Larger values correspond to circumferential modes in the radial transmission line. Calculation of the higher order resonant wavelengths corresponding to radial modes in the transmission line are more complex but not important to the present discussion.

Because of the coupling to the cathode structure mentioned previously the resonance wavelength is very strongly dependent upon the details of cathode circuit. If these details are known so that the coupling to and the impedance of the cathode circuit can be calculated, the effect on resonance wavelength can be predicted. Results of cold tests made on a brass model of an interdigital magnetron are shown in Figure 23. The resonant wavelength of the structure is tuned from 15 to 18.5 cm. by moving plugs short circuiting between a dummy cathode stem and the outer cylinder extending both ways from the bases of the anode teeth. For the

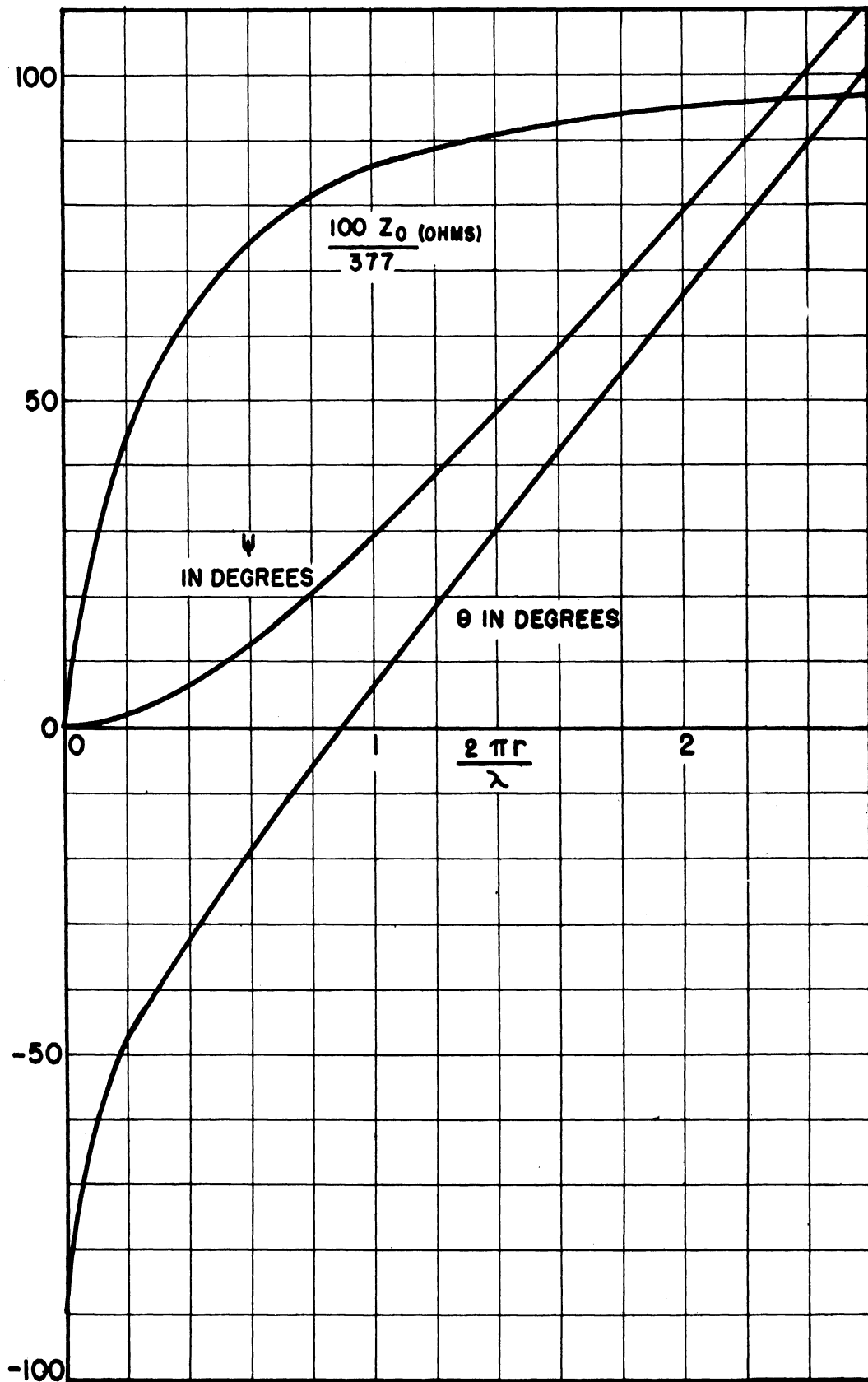


FIG. 22 RADIAL TRANSMISSION LINE QUANTITIES

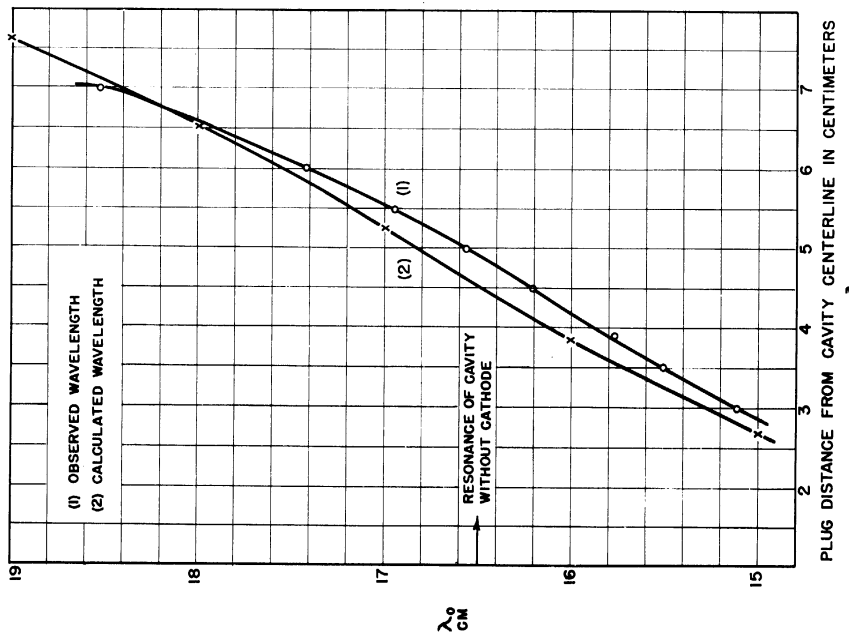
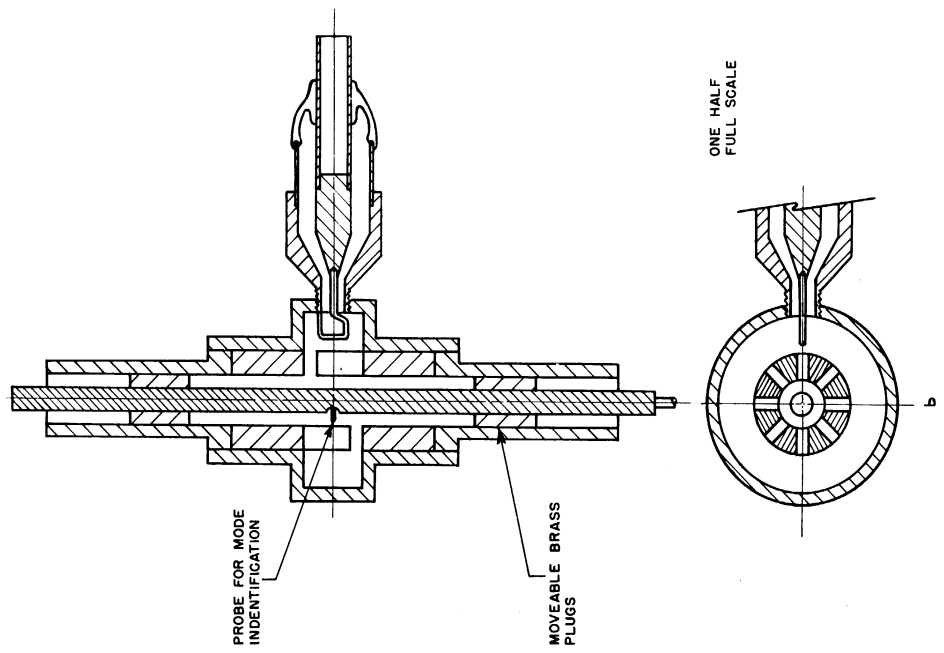


FIG. 23 a
EFFECT OF SHORT CIRCUITING PLUGS IN CATHODE LINE
ON RESONANT WAVELENGTH OF INTERDIGITAL MAGNETRON



MODEL USED IN MEASUREMENTS SHOWN IN FIG. 23 a

FIG. 23 b
TUNING EFFECT OF SHORT CIRCUITING PLUGS IN CATHODE LINE

calculated curve the cathode circuit was considered a short-circuited coaxial transmission line coupled to the resonant cavity by the capacitance of the interdigital anodes. The results of these measurements and calculations made on simple structures of this type lead to the suggested design for a frequency modulatable magnetron shown in Figure 24. In this structure the effective length of the transmission line formed by the cathode and the cathode by-pass sleeves is varied by the presence of a magnetron space charge of the type described in the preceding sections. The dielectric constant of the space charge is given by the curves in Figure 19b since propagation in the modulator structure is in the direction of the axial magnetic field. A magnetron of this type is being constructed at the University of Michigan. The modulator portion of the structure is a simple diode and should cause no difficulty as a source of parasitic oscillations.

The choice of the interdigital magnetron for the development was made purposely because it appeared to have more possibilities than the vane-type in a double anode structure. The interdigital anodes at the same time provide the capacitance portion of the resonant circuit and the multianode structure required for magnetron oscillation. The resonant circuit itself is simple in geometry and not necessarily restricted to the type used in the conventional interdigital magnetron. The radial transmission line structure may conceivably be replaced by any section of transmission line or other structure which will resonate with the capacitance of the anode teeth at a frequency capable of excitation by the electrons in the interaction space. The vane-type magnetron, on the other hand, is very complex in geometry. The vanes supply both capacitance and inductance to the resonant circuit. Two sets of anodes almost assuredly

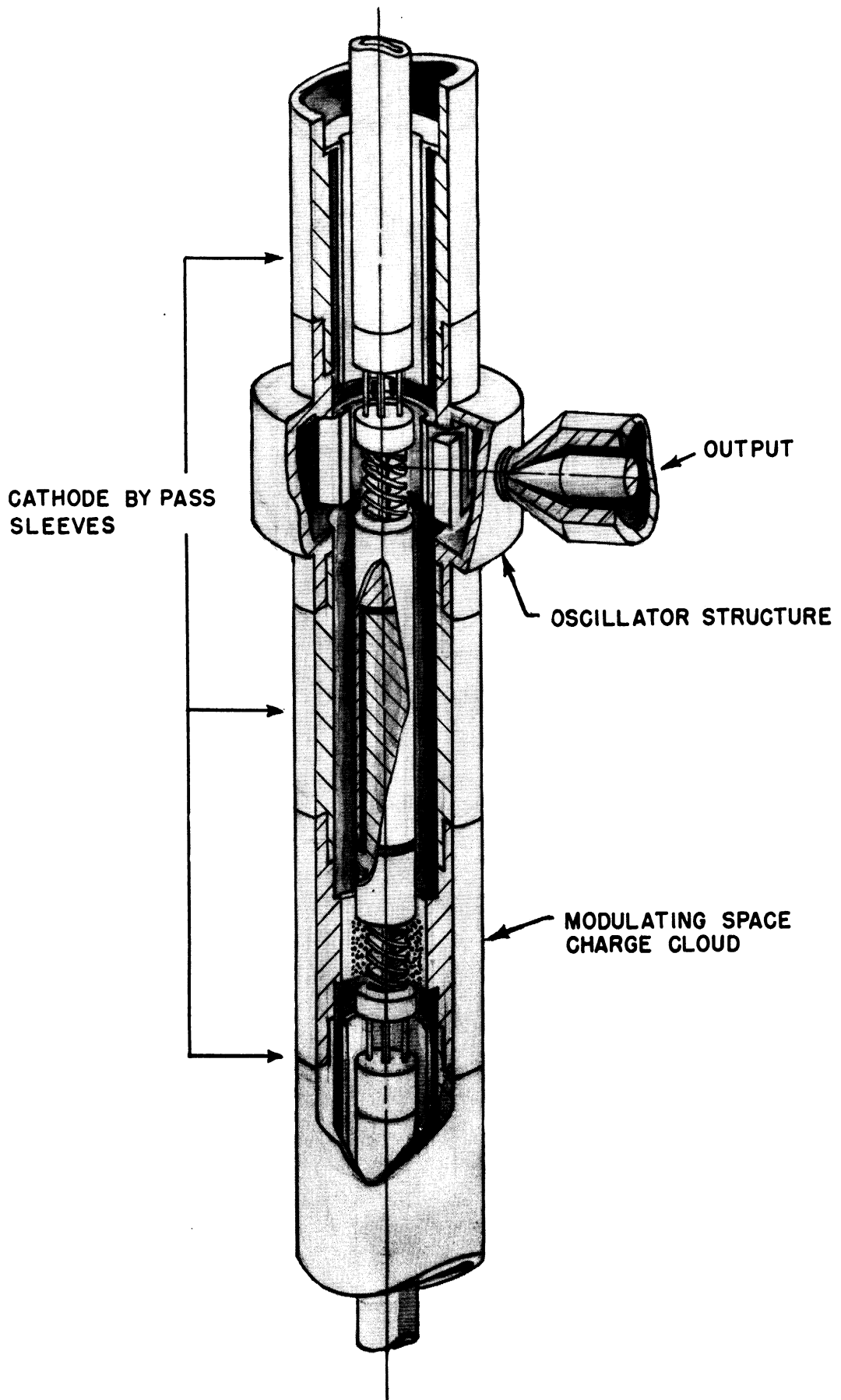


FIG. 24 FREQUENCY MODULATION INTERDIGITAL MAGNETRON

will mean complex resonances.

Four possibilities are shown schematically in Figure 25. These structures are meant only to be illustrative of the manner in which interdigital anodes might be used in frequency modulated magnetrons. In order to make them practicable, problems of cooling, tuning and mechanical construction must be solved. In all of the devices an axial magnetic field is assumed present.

The structure shown in Figure 25a is mechanically possible and easily cooled. Modulation would be obtained by varying the voltage on the modulator cathode. Preliminary measurements have been made on a brass model of a resonant cavity for this type. The findings indicate that the modes are not as nicely separated as in the cavity used with the ordinary interdigital magnetron oscillator.

The mode separation in the type pictured in Figure 25b should be good. Methods for supporting and cooling the inner sets of anodes without spoiling mode separation will have to be worked out to make this type practical. The use of resonant stub supports is inadvisable but may be necessary. Modulation would again be obtained by varying the voltage or the modulator cathode.

The device pictured in Figure 25c is conceivable but probably the least practicable of the group. Cooling and supporting the inner anode and isolating the cathode for modulation purposes are all difficult problems.

The grid structure shown in Figure 25d is very speculative but might be feasible. A rugged second grid could provide support and a cooling channel for the inner set of anodes. The grid structures would necessarily operate in a low magnetic field and at close spacings; otherwise

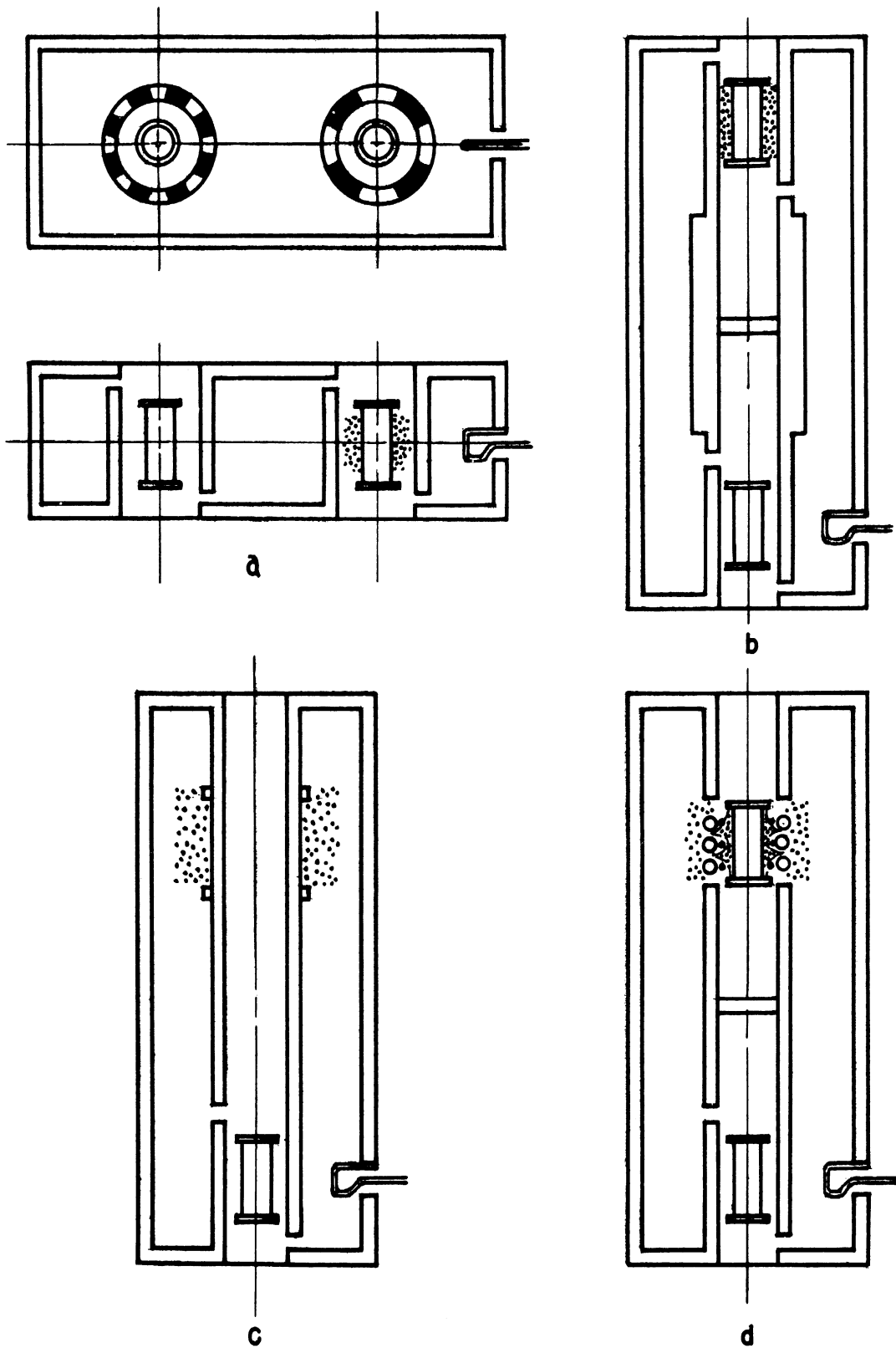


FIG. 25 POSSIBILITIES OF INTERDIGITAL ANODE STRUCTURES IN FREQUENCY MODULATION MAGNETRONS

NOTE: SPACE CHARGE CLOUD IS SHOWN IN MODULATION ANODES ONLY

electrons could not traverse the grids. The electrons would be injected into the cavity with an initial velocity rather than continuously extracting energy from the d-c field. A space charge would thus be formed in the coaxial cavity similar to that developed in the magnetron. The mathematics of this case has not been worked out but it is fairly obvious that the amount or extent of the space charge could be controlled by the grids. The second grid or the outside of the cavity could act as a collector. The proximity of the magnetron oscillator structure requiring high magnetic field provides a limitation which might prevent the arrangement of the structures indicated in the drawing. The grid structure modulator might be more adaptable to use in the reactance tube type of modulation.

Variations of these geometries are being considered as well as other possibilities. At least one type of multianode modulator structure will be built in this laboratory in order to compare the results with the smooth-bore anode structure of the type in Figure 24. The number of anodes, the design of the interaction space and the magnetic field to be used will be selected to test the design formulae given in Section 8.

10. CONCLUSIONS

The subject matter and objectives of this report are summarized in the introduction. This report is not meant to be a complete and final analysis of the problem of the magnetron space charge and frequency characteristics. It is intended to relate as many as possible of the known facts and theories in such a way that it can be used as a guide for further research and development. We have presented in some detail the ideas and

data originating in the University of Michigan laboratory and have given a fairly complete bibliography of other sources. We have tried to provide enough discussion and criticism of other ideas to make the development consistent.

Some important conclusions have been mentioned in the discussion of the experimental results and theory. These are the following:

(a) The unpredicted plate current which is drawn before the Hartree or Hull boundaries are reached may be related to the high noise levels observed in the magnetron.

(b) Frequency pushing with increasing voltage is primarily due to a decrease in wavelength caused by the active phasing effect of the electrons in the spokes of the space charge wheel acting as a current generator in the magnetron.

(c) Frequency shifts with increasing voltage under hot-impedance test conditions are primarily of two types. Both are due to passive effects of the space charge in the space-charge wheel. In one case, $\omega_f < .36 \omega_c$, the dielectric constant of the hub of the space-charge wheel is negative and the resonant wavelength increases as the hub expands. In the other case, $\omega_f > 1.36 \omega_c$, the dielectric constant of the hub of the space-charge wheel is positive but less than unity and the wavelength decreases as the hub expands.

(d) For a particular value of magnetic field, under hot impedance test conditions, the natural resonance of the individual electrons in the space charge causes large frequency shifts. This is the cyclotron resonance ($\omega_f = \omega_c$).

(e) Frequency pulling is primarily an effect of circuitry.

Deviations from the values predicted on the basis of circuitry are due to interrelation of the equivalent susceptance and conductance of the space-charge cloud acting as a current generator in the magnetron. They are therefore related to frequency pushing.

(f) Frequency shifts of the type mentioned in (c) may be used to obtain frequency modulation.

It would be possible to amplify experience by carrying out some of the experiments suggested in Section 3. The exact value of y_e , the electronic admittance, could be calculated from experimental data on a particular magnetron for either the non-oscillating or oscillating case. Possibly, if enough data were available on different magnetrons, generalizations could be made which would give more insight into the actual behavior in the oscillating magnetron. The theory has reached the point, however, where a more refined analysis than has been given thus far is necessary to improve upon the present picture. A true quantitative explanation of the details of the Rieke diagram and frequency pushing curves can only result from such an analysis.

However, the results we have, used carefully with due regard for the underlying assumptions, are sufficient to provide basis for development of frequency modulation devices along lines of thought similar to those suggested in Sections 8 and 9. Care must be exercised that the limited available knowledge of underlying principles of behavior does not limit unnecessarily the flexibility of approach to the problem of frequency modulation. The magnetron itself was founded on very general principles and has been working quite well for several years in spite of

our inability to understand the details of its operation.

Two very important problems have not been discussed. These are the problems of frequency stabilization and noise reduction⁽¹⁾. Both are essential to successful usage of c-w magnetrons for communication. The former we believe to be a problem of circuitry once an electronic control on frequency is provided. It is essential to use a monitoring method since low Q is required in the oscillator resonant circuit to obtain wide band modulation. Where modulation is not necessary it is sometimes possible to use a high- Q stabilizing cavity coupled directly to the magnetron. A clue to the noise problem may be given in the association of noise output with the pre-Hull voltage plate current mentioned in Section 7. However, the experimental data are inadequate and should be supplemented. In view of the complex nature of noise production and the possibility of noise amplification, the experimental statistical approach will probably be more fruitful in the immediate future than the theoretical approach.

The problem of linearity of modulation and other problems having essentially to do with circuitry cannot be discussed adequately until data are available on some operating frequency-modulation magnetrons.

(1) X.

BIBLIOGRAPHY

The references in the following list were all influential in one way or another to the development of the present report. There are other references which are undoubtedly important which the author did not have opportunity to read. Because of the varied subject matter the references are arranged under headings corresponding to the text for which they are most useful. Footnote references are only given for specific information.

I. General

1. University of Michigan Electron Tube Laboratory Staff, Monthly Progress Reports, July 1946 to September 1948. Project M694, Contract No. W36-039 sc-32245.
2. Peters, P. H., Magnetron Modulation, Quarterly Progress Reports No. 1 to No. 7, October 1946 to April 1948, General Electric Company, Contract No. W36-039 sc-32279.
3. Slater, J. C., Theory of the Magnetron Oscillator, Radiation Laboratory Report No. V5S (118), August 1941.
4. Slater, J. C., Theory of Magnetron Operation, Radiation Laboratory Report 43-28 (200), March 8, 1943.
5. Fisk, J. B., Hagstrum, H. D. and Hartman, P. L., The Magnetron as a Generator of Centimeter Waves, Bell System Technical Journal, Vol. XXV, No. 2, April 1946.
6. Radiation Laboratory Series, Microwave Magnetrons, McGraw Hill, New York, Toronto, London, 1948.
7. Radio Research Laboratory Staff, Very High Frequency Techniques, Vol. I and II, McGraw Hill, New York and London, 1947.

8. Bothwell, F. E. and Crout, P. D., A Method for Calculating Magnetron Resonant Frequencies and Modes, Radiation Laboratory Report No. 1039, February 8, 1946.

II. Equivalent Circuit

1. Rieke, F. F., Analysis of Magnetron Performance, Part I, Equivalent Circuit Method, Applications, Radiation Laboratory Report 52-10 (229), September 16, 1943.
2. See: I-4, 5, 6, 7

III. Experimental Evidence of Space-Charge Effects on Frequency Characteristics

1. Radiation Laboratory Series, Technique of Microwave Measurements, McGraw Hill, New York and London, 1947.
2. Platzman, R., Evans, J. E. and Rieke, F. F., Analysis of Magnetron Performance, Part II, Detailed Study of the Operation of a Magnetron, Radiation Laboratory Report No. 451, March 3, 1944.
3. Turnbull, J. C., Duggan, J. R., Otis, C. F. and Welch, H. W., Modulation Tests of the 6J21 Magnetron, Radio Research Laboratory Report No. 411-235, October 29, 1945.
4. See: I-4, 5, 6, 7
VI-2, 3

IV. Space Charge and the Equivalent Circuit

1. See: I-5, 6, 7
II-1

V. Analysis of Space-Charge Behavior in the Magnetron

1. Brillouin, L., Theory of the Magnetron I, Physical Review, Vol. 60, 385-396, September, 1941.
2. Allis, W. P., Theory of the Magnetron Oscillator, Electronic Orbits in the Cylindrical Magnetron with Static Fields, Radiation Laboratory Special Report 95, Section 5 (122), 1941.
3. Allis W. P., Outline for a Theory of the Space Charge in an Oscillating Magnetron, Radiation Laboratory Report 43-3 (176), 1942.

4. Hartree, D. R., Estimates of Electron Energies, Oscillation Amplitudes, and Efficiencies in a Magnetron Operating Under Rotating Space Charge Conditions, C.V.D. Report, Ref. Mag. 11.
5. Bloch, F., Space Charge Limited Single-Stream Solutions in a Cylindrical Magnetron with Small Current, Radio Research Laboratory Report No. 411-175, May 25, 1945.
6. Vineyard, G., A Numerical Calculation of Space Charge Behavior and Power in the Magnetron, Radiation Laboratory Report No. 43-29 (201), March 29, 1943.
7. See: I-3, 5, 6

VI-1

VI. Propagation of Electromagnetic Wave in Magnetron Space Charge

1. Blewett, J. P., and Ramo, S., High Frequency Behavior of a Space Charge Rotating in a Magnetic Field, Physical Review, Vol. 57, 635-641, April, 1940.
2. Blewett, J. P., and Ramo, S., Propagation of Electromagnetic Waves in a Space Charge Rotating in a Magnetic Field, Journal of Applied Physics, Vol. 12, 856, 1941.
3. Lamb, W. E., Jr., and Phillips, M., Space Charge Frequency Dependence of Magnetron Cavity, Journal of Applied Physics, Vol. 18, 230-238, February 1947.
4. King, R. W. P., Electromagnetic Engineering, Vol. I, Fundamentals, McGraw Hill, New York, London, 1945.
5. Stratton, J. A., Electromagnetic Theory, McGraw Hill, New York and London, 1941.
6. Mimno, H. R., The Physics of the Ionosphere, Review of Modern Physics, Vol. 9, No. 1, 1-68, January 1937. Excellent list of references given in this article to papers on propagation in space charge.

VII. Discussion of Space-Charge Behavior and Interpretation of Experimental Evidence

See: I-4, 5, 6, 7

II-2

V-1, 3, 4, 5

VI-2, 3

VIII. General Discussion of Frequency Modulation

1. R.C.A. Laboratories, Reactance Tube Frequency Modulation of Microwave Oscillators, Report No. 20 of Contract No. NX sa 35042.
2. Smith, L. P. and Shulman, C. I., Frequency Modulation and Control by Electron Beams, Proceedings of the IRE, Vol. 35, No. 7, 644-657, July 1947.
3. Kilgore, G. R., Shulman, C. I. and Kurshan, J., A Frequency Modulated Magnetron for Super High Frequencies, Proc. IRE, Vol. 35, No. 7, 657-664, July 1947.
4. Donal, J. S., Jr., Bush, R. R., Cuccia, C. L. and Hegbar, H. R., A 1-Kilowatt Frequency Modulated Magnetron for 900 Megacycles, Proc. IRE, Vol. 35, No. 7, 664-669, July 1947.
5. Saxon, D. S., General Theory of Electronic Beam Modulators, Radiation Laboratory Report No. 758, March 15, 1946.
6. Banos, A., Jr. and Saxon, D. S., An Electronic Modulator for C-W Magnetrons, Radiation Laboratory Report 748, June 26, 1945.
7. R.C.A. Laboratories, The Diode Frequency Modulator, Report No. 16 of Contract NX sa 35042, December 1, 1944.

IX. Suggested Geometries for Frequency Modulation Magnetrons

1. Crawford, F. H. and Hare, M. D., A Tunable Squirrel Cage Magnetron-The Donutron, Proc. IRE, Vol. 35, No. 4, 361-369, April, 1947.
2. Hare, M. D. and Leonard, Virginia, The Construction of the Donutron, A Tunable Squirrel Cage Magnetron, Radio Research Laboratory Report No. 411-249, October 26, 1945.
3. Hull, J. F. and Randalls, A. W., A High Power Interdigital Magnetron, ESM-15, Engineering Report No. E-1015, Signal Corps Engineering Laboratories, Fort Monmouth, New Jersey, October 29, 1947.
4. Hull, J. F., Mathematical Treatment of Modes in the Squirrel Cage Interdigital Magnetron, E.S.L. Memo for File, Nov. 21, 1946.
5. Ramo, S., Whinnery, J. R., Fields and Waves in Modern Radio, John Wiley, New York, Chapman and Hall, London, 1944.

X. Miscellaneous

1. Sproull, R. L., Excess Noise in Cavity Magnetrons, Journal of Applied Physics, Vol. 18, No. 3, 314-320, March 1947.

2. Mayper, V., Noise Generation in Pre-Oscillating Magnetron, Quarterly Progress Report, M.I.T. Research Laboratory of Electronics, 4-6, January 15, 1948.
3. Norton, L. E., Frequency Stabilization of Oscillators by a Method Particularly Adapted to the Higher Frequencies and Magnetron Sources, R.C.A. Laboratories Report No. 13008 on Contract No. OEM-sr-684, May 1944.
4. Helber, C. A., An Automatic Frequency Control and Frequency Selection System for Magnetrons, Radiation Laboratory Report No. 541, April 1944.
5. Hollingsworth, L. M. and Dickinson, R., An Automatic Frequency Control System for Magnetrons with Beacon Application, Radiation Laboratories Report No. 1020, March 9, 1946.
6. Pound, R. V., An Electronic Frequency Stabilization System for C-W Microwave Oscillators, Radiation Laboratory Report No. 815, October 1945.
7. Pound, R. V., A Microwave Frequency Discriminator, Radiation Laboratory Report No. 662, August 1945.
8. Smith, W. V., Herlin, M. A. and Weightman, H. G., XCT Final Report, Radiation Laboratory Report No. 879, March 1946 (Electronic Tuning).
9. Donal, J. S., Jr., Cuccia, C. L., Brown, B. B., Vogel, C. P. and Dodds, W. J., Stabilized Magnetron for Beacon Service, R.C.A. Review, Vol. III, No. 2, 352-372, June 1947.

DEFINITION OF SYMBOLS

Units are in rationalized MKS system except where noted in experimental data given in the report.

<u>Symbol</u>	<u>Definition</u>	<u>Units</u>
\vec{B}	vector value of magnetic field	webers/sq m
B, B_z	z-component of static magnetic field	webers/sq m
B_n	value of magnetic field for which outermost electrons are in synchronism with r-f field	webers/sq m
B_o	value of magnetic field for which electrons just reach synchronous angular velocity at the magnetron anode	webers/sq m
b_e	susceptance of space-charge cloud as seen from magnetron anodes	mhos
B_L	susceptance of load of magnetron as transformed to magnetron anodes	mhos
B_T	total susceptance of tank circuit as seen from magnetron anodes	mhos
c-w	continuous wave	
C	capacitance in equivalent circuit for magnetron (also constant of integration)	farads
C_a	anode capacitance interdigital magnetron	farads
C_c	capacitance from anode to cathode in magnetron	farads
d	spacing between anode fingers in interdigital magnetron	m
e_T	r-f voltage in equivalent circuit for magnetron	volts
E	electrical potential	volts

<u>Symbol</u>	<u>Definition</u>	<u>Units</u>
E'	potential at an arbitrary point in charge free space within the magnetron anode	volts
E_a	potential at anode of magnetron	volts
E_{an}	potential at anode of magnetron for which outermost electrons are in synchronism	volts
E_c	cathode potential - usually considered = 0	volts
E_n	potential drop which must have been experienced by outermost electrons traveling at synchronous angular velocity	volts
E_o	value of anode potential for which electrons just reach synchronism at the anode	volts
f	frequency = $2\pi c/\lambda$	cycles/sec
f-m	frequency-modulation	
\vec{F}	electric field strength	volts/m
F_r	r-component of electric field strength	volts/m
F_θ	θ -component of electric field strength	volts/m
\vec{F}_o	amplitude of electric field vector in r-f wave	volts/m
g_e	conductance of space-charge cloud as seen from the anodes	mhos
G_L	conductance of load as transformed to magnetron anodes	mhos
G_o	characteristic conductance of resonant circuit as seen from the load = Y_o/σ_o	mhos
G_T	internal conductance of magnetron equivalent circuit	mhos
h	height of cavity in interdigital magnetron	m
H	magnetic field component of electromagnetic wave	amp/m
i_e	r-f current delivered to space-charge cloud from anodes of magnetron	amp
i_T	r-f current delivered to tank circuit from anodes of magnetron	amp

<u>Symbol</u>	<u>Definition</u>	<u>Units</u>
i_g	r-f current generated by rotating space charge in oscillating magnetron	amp
I_a	anode steady state current	amp
K	constant of proportionality determining capacitance between anode and cathode in magnetron	
l	length of finger in interdigital magnetron	m
L	inductance in magnetron equivalent circuit (also used as length of magnetron cathode in Table 1)	henries
L_M	distance from magnetron output to a minimum in cold test measurements	m
M	mutual inductance of coupling loop and magnetron tank inductance in equivalent circuit	henries
N	number of anodes in magnetron	
n	mode number in oscillating magnetron = $N/2$ for π -mode	
Q	ratio of stored energy to lost energy in resonant circuit	
Q_o	ratio of stored energy to internally lost energy in resonant circuit	
Q_L	ratio of stored energy to combined internally and externally delivered energy in resonant circuit	
r	radial distance in cylindrical coordinate	m
r_a	radius of magnetron anode	m
r_c	radius of magnetron cathode	m
r_H	radius of Hull space charge cloud	m
r'	radial location of arbitrary point in charge free space within magnetron anodes	m
r-f	radio-frequency	
\vec{r}_1	unit vector in r-direction	
R_a	outer radius of interdigital magnetron anodes	m

<u>Symbol</u>	<u>Definition</u>	<u>Units</u>
R_c	inside radius of outer cavity wall in inter-digital magnetron	m
s	thickness of sheath of electrons surrounding cathode	m
\vec{v}	vector value of velocity of electron	m/sec
v_r	radial component of electron velocity	m/sec
y_e	admittance of space-charge cloud as seen from magnetron anodes	mhos
Y_L'	admittance of magnetron load at output terminals	mhos
Y_L	admittance of load as transformed to magnetron anodes	mhos
Y_0	characteristic admittance of line	mhos
Y_{oc}	$\sqrt{\frac{C}{L}}$ = characteristic admittance of equivalent circuit	mhos
Z_{el}	$\frac{F\theta}{H}$ = impedance of electron cloud in magnetron	ohms
Z_0	characteristic impedance of line	ohms
Z_{oa}	characteristic impedance of radial transmission line at R_a	ohms

Greek Letters

α	ratio of anode to cathode capacitance to total equivalent capacitance of magnetron anodes = C_c/C_a	
ϵ_r	relative dielectric constant	
$\vec{\theta}_1$	unit vector in θ -direction cylindrical coordinates	
θ	function of $2\pi r/\lambda$ used in determination of radial transmission line input impedance	degrees
θ_a	θ defined at R_a	degrees

<u>Symbol</u>	<u>Definition</u>	<u>Units</u>
θ_c	θ defined at R_c	degrees
λ	wavelength	m
λ_0	resonant wavelength	m
ρ	space-charge density	coulombs/m ³
σ	complex conductivity	mhos
σ_0	minimum standing wave ratio in impedance test	
τ	total space charge per unit length in magnetron	coulombs/m
ψ	function of $2\pi r/\lambda$ used in determination of radial transmission line input impedance	degrees
ψ_a	ψ defined at R_a	degrees
ω	angular velocity of electron in magnetron	radians/sec
ω_c	= Be/m = angular frequency of natural resonance of the electrons	radians/sec
ω_f	= $2\pi f$, angular frequency of oscillation	radians/sec
ω_L	= $Be/2m$ = maximum angular velocity the electron can have in a magnetron under static conditions	radians/sec
ω_n	= ω_f/n = angular velocity of traveling r-f wave in magnetron for n-th mode	radians/sec
ω_0	cold angular resonance frequency of magnetron	radians/sec

Physical Constants and Conversions

c	velocity of radiation in free space = 2.99×10^8 m/sec
e	electronic charge = 1.6×10^{-20} e.m.u. = 1.6×10^{-19} coulombs
m	electronic mass = 9.1×10^{-31} kgm.

<u>Symbol</u>	<u>Definition</u>
e/m	specific charge of electron = 1.759×10^7 e.m.u./gm. = 1.759×10^{11} coulombs/kgm.
ϵ_0	dielectric constant of free space = $\frac{1}{36\pi} \times 10^{-9}$ farads/m
	1 weber/sq m = 10^4 gauss

UNIVERSITY OF MICHIGAN



3 9015 02526 5524